JCB Journal of Cell Biology

ARTICLE

A cell separation checkpoint that enforces the proper order of late cytokinetic events

Jennifer L. Brace, Matthew D. Doerfler, and Eric L. Weiss

Eukaryotic cell division requires dependency relationships in which late processes commence only after early ones are appropriately completed. We have discovered a system that blocks late events of cytokinesis until early ones are successfully accomplished. In budding yeast, cytokinetic actomyosin ring contraction and membrane ingression are coupled with deposition of an extracellular septum that is selectively degraded in its primary septum immediately after its completion by secreted enzymes. We find this secretion event is linked to septum completion and forestalled when the process is slowed. Delay of septum degradation requires Fir1, an intrinsically disordered protein localized to the cytokinesis site that is degraded upon septum completion but stabilized when septation is aberrant. Fir1 protects cytokinesis in part by inhibiting a separation-specific exocytosis function of the NDR/LATS kinase Cbk1, a key component of "hippo" signaling that induces mother–daughter separation. We term this system enforcement of cytokinesis order, a checkpoint ensuring proper temporal sequence of mechanistically incompatible processes of cytokinesis.

Introduction

Eukaryotic cells reproduce through interlaced, mechanistically diverse events that happen with specific relative timing. This sequential order can be crucial: in some cases, productive division requires dependency relationships in which late events are not initiated until specific early processes are fully completed, even though these late events do not inherently require the early ones (Hartwell, 1971). Anaphase separation of chromosomes, for example, must not begin until DNA replication is complete and kinetochores are appropriately attached to the mitotic spindle, and cells must not physically divide before the duplicated genome has been partitioned. To ensure these dependencies, eukaryotic cells have evolved regulatory mechanisms known as checkpoints that actively block downstream events until upstream ones are successfully finished (Hartwell and Weinert, 1989; Li and Murray, 1991; Khodjakov and Rieder, 2009). These systems effectively monitor the status of key processes, generating negative signals that impede progression to later stages until specific biochemically sensed criteria are satisfied. For example, unattached kinetochores produce an inhibitor that blocks destruction of mitotic cyclin and thus prevents the metaphase–anaphase transition (reviewed in Musacchio, 2015). Importantly, checkpoint-monitored processes lose sequential dependencies when checkpoint mechanisms are nonfunctional, a disruption that is especially problematic when early events are themselves disrupted. The spindle assembly and DNA damage checkpoints are well studied, and it is becoming clear that additional checkpoint-like mechanisms protect the integrity of cell division. For example, failure to successfully complete cytokinesis in higher eukaryotes induces a checkpoint-like response that prevents tetraploidization (Steigemann et al., 2009), and cells with lagging chromosomes actively block cytokinesis that would cause chromosome damage (Norden et al., 2006; Mendoza et al., 2009; Nähse et al., 2017).

Eukaryotic cells undergo dramatic reorganization at the end of mitosis, producing two cells from one through the processes of cytokinesis. This division requires execution of mechanistically diverse events in an unvarying and often rapid sequence. Specification of the division site and assembly of cytokinetic structures precede the mechanical and regulatory events of actomyosin ring (AMR) constriction and membrane ingression; this is followed by disassembly of cytokinetic machinery, cessation of cytokinetic membrane trafficking, and abscission of the divided cells (Green et al., 2012; Mierzwa and Gerlich, 2014; Gould, 2016; Glotzer, 2017). In some cases, the relative timing of cytokinesis events may reflect inherent structural dependencies, but overall the mechanisms that enforce the temporal sequence of cytokinesis phases are not well understood.

Cytokinesis in the budding yeast *Saccharomyces cerevisiae* proceeds through a rapid sequence of processes that are broadly conserved (reviewed in Balasubramanian et al., 2004; Weiss, 2012; Juanes and Piatti, 2016; Bhavsar-Jog and Bi, 2017), including

Department of Molecular Biosciences, Northwestern University, Evanston, IL.

Correspondence to Eric L. Weiss: elweiss@northwestern.edu.

https://doi.org/10.1083/jcb.201805100

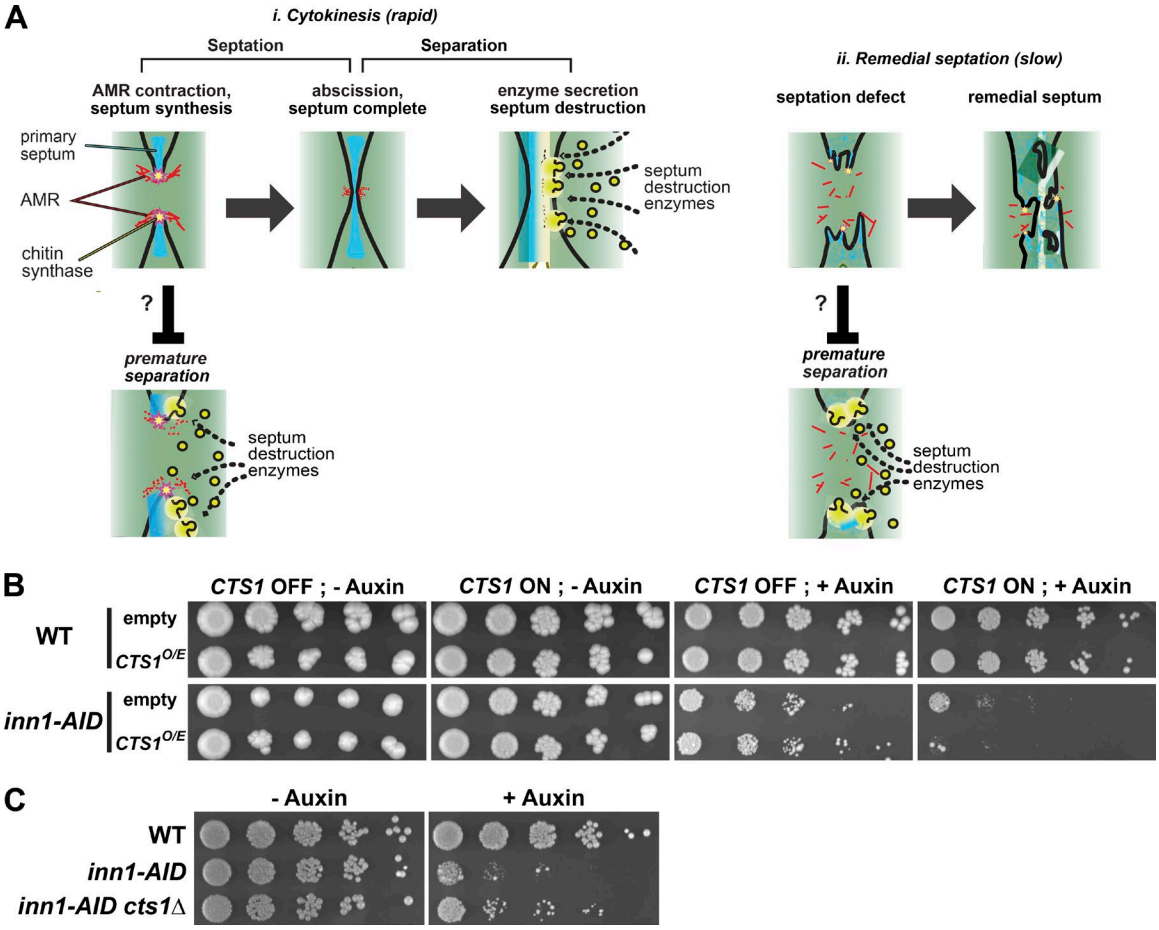

Figure 1. **Septation mutants are sensitive to inappropriate activation of cell separation. (A)** Cytokinesis in budding yeast. i: Normal, rapid cytokinesis can be separated into two broad phases: septation and cell separation. Only after completion of septation are septum-destroying enzymes secreted. To ensure this temporal order, we predict cells actively inhibit separation until septation is complete. ii: Cells with septation defects generate a remedial septum. Cells forming a slow remedial septum are particularly sensitive to premature septum degradation, and we propose cells activate a checkpoint-like mechanism to enforce the strict temporal order of septation and separation. **(B)** Inappropriate *CTS1* expression is detrimental when septation fails. WT and *inn1-AID* cells transformed with an empty vector or a galactose-inducible vector expressing *CTS1* were spotted in fivefold serial dilutions to plates containing glucose (*CTS1* OFF) or galactose (*CTS1* ON). Additionally, the plates contained 0.5 mM auxin (+Auxin) or DMSO (−Auxin). Plates were incubated at 30°C for 3 d. All strains express the E3 ligase *TIR1*. **(C)** *CTS1* deletion partially restores viability to cells with disrupted septum synthesis. The indicated strains were grown on YPD plates containing 0.5 mM auxin (+Auxin) or DMSO (−Auxin) and incubated at 30°C for 3 d. All strains express the E3 ligase *TIR1*.

AMR construction and constriction, highly localized membrane addition, and membrane abscission (Fig. 1 A i). Like many eukaryotes, budding yeast cells build a specialized extracellular barrier called the septum at the site of cytokinesis: in general, free-living cells like budding yeast are under extreme turgor pressure, and the septum is thus critical for osmotic integrity during the division process (Levin, 2005; Cortés et al., 2012; Proctor et al., 2012). Exemplifying the complex, multi-system coordination needed for successful cytokinesis, septum construction in budding yeast is temporally and spatially controlled. Mitotic exit network (MEN; reviewed in Meitinger et al., 2012) activation triggers AMR localization of proteins, which activate primary septum synthesis by the membrane-spanning chitin synthase at the ingressing division furrow (VerPlank and Li, 2005; Zhang et al., 2006; Nishihama et al., 2009; Meitinger et al., 2010; Chin et al., 2012; Oh et al., 2012; Palani et al., 2012; Kuilman et al., 2015). As the AMR-guided chitin septum forms, it is followed by localized production of glucan-rich secondary septa on both the mother and daughter cell sides (Cabib, 2004; Lesage and Bussey, 2006). While mechanisms that coordinate the timing of primary and secondary septum production are incompletely understood, recent analyses demonstrate coordinated regulation ensures the appropriate order of these distinct processes (Atkins et al., 2013; Meitinger et al., 2013; Onishi et al., 2013; Oh et al., 2017).

Remarkably, the septum is destroyed only minutes after it is completed. Once septation is complete, daughter cells secrete degradative enzymes to destroy the primary septum and release daughter cells from their mothers (Fig. 1 A i). A "hippo" signaling pathway called the regulation of Ace2 and morphogenesis (RAM) network controls this process (reviewed in Weiss, 2012). Mutants in this pathway exhibit defects in cell separation and accumulate as large clumps of cells (Weiss et al., 2002; Nelson et al., 2003; Kurischko et al., 2005). The downstream most kinase, Cbk1, is critical to direct the cell separation process (Bidlingmaier et al., 2001; Colman-Lerner et al., 2001; Weiss et al., 2002; Jansen et al., 2006). In late mitosis, Cbk1 is activated upon MEN-dependent

release of the phosphatase Cdc14 and activates the transcription factor Ace2 (Brace et al., 2011). Cbk1 interacts with Ace2 through a recently discovered docking motif (Nguyen Ba et al., 2012; Gógl et al., 2015) and phosphorylates the transcription factor Ace2 at its nuclear export sequence, trapping the protein in the daughter cell nucleus (Mazanka et al., 2008). There, Ace2 drives transcription of genes required to efficiently degrade the septum (Colman-Lerner et al., 2001). One such gene encodes the endochitinase Cts1, a secreted protein that degrades chitin in the primary septum, leading to cell separation (Elango et al., 1982; Kuranda and Robbins, 1991); however, any regulation on Cts1 secretion is yet unknown.

It is unclear how—or if—degradation of the septum is coupled to its successful synthesis. Interestingly, Ace2 localizes to the daughter cell nucleus before the completion of septation, and transcription of Cts1 and other cell separation genes begins before cytokinesis (Mazanka et al., 2008). Thus, precytokinetic cells could be capable of producing Cts1 and other degradative enzymes, even though premature degradation of the forming structure would likely be detrimental to the dividing cell (Cabib et al., 1992). Thus, we hypothesized that a checkpoint mechanism forestalls separation processes until completion of septation (Fig. 1 A). To better understand mechanisms that enforce cytokinesis order, we investigated the coupling of septation and mother–daughter separation in yeast cytokinesis. Our findings indicate that a checkpoint mechanism prevents secretion of Cts1, and thus degradation of the septum, when early cytokinetic processes important for septum formation are defective. This pathway involves the protein Fir1, a probable RAM network target that is normally degraded after AMR constriction but persists at the cytokinesis site when septation is defective. In the absence of Fir1, cells with septation defects prematurely secrete Cts1 and fail to complete cytokinesis normally. We term this checkpoint-like mechanism the enforcement of cytokinesis order (ECO) pathway.

Results

For clarity, we refer to the combined processes of AMR contraction, membrane ingression, septum construction, abscission, and septum degradation as "cytokinesis" (Fig. 1 A). We divide cytokinesis into two broad phases: "septation" beginning with AMR contraction/septum construction and ending with septum completion, and "separation" beginning with secretion of Cts1 and other enzymes and ending with full degradation of the extracellular mother–daughter junction, the primary septum, and release of both cells (Fig. 1 A i). In budding yeast, these events happen in rapid succession, leading to production of two completely separated cells in ∼10 min under normal growth conditions.

Cells with septation defects are sensitive to artificial changes in Cts1 levels

We sought to determine if cells enforce dependency of late stages of cytokinesis on successful completion of early ones. The protein Inn1 links the AMR to machinery that extrudes chitin polymer into the extracellular space (Sanchez-Diaz et al., 2008; Meitinger et al., 2010; Devrekanli et al., 2012) and is crucial for successful early cytokinesis. Cells lacking Inn1 cannot perform actomyosin-directed septum formation, and instead deposit a disorganized remedial septum composed of chitin and other extracellular glucans at the bud neck that eventually closes off the cytoplasmic connection between mother and daughter cells (Nishihama et al., 2009; Fig. 1 A ii). We used an auxin-inducible degron (AID) system (Nishimura et al., 2009) to conditionally deplete Inn1 and disrupt normal septation. We found that, as reported, cells carrying the *inn1-AID* allele produce a functional Inn1-AID fusion protein that is rapidly degraded in the presence of the exogenous ubiquitin ligase Tir1 and auxin (Devrekanli et al., 2012), with attendant failure of mother–daughter separation (Fig. S1, A and B; Sanchez-Diaz et al., 2008; Nishihama et al., 2009).

The process of mother–daughter separation is directly antagonistic to septation. If separation does not inherently require septum completion to proceed, then enhancing its cell separation activity might worsen phenotypes associated with septation defects. Conversely, elimination of its cell separation activity might ameliorate them. We therefore overexpressed the cell separation chitinase Cts1 in cells with defective early cytokinetic processes, placing *CTS1* under the control of a galactose-inducible promoter and again using auxin treatment of *inn1-AID* cells to induce defective septation. We found that *inn1-AID* cells grew poorly but measurably in the presence of auxin, while no growth occurred in combination with the *CTS1* overexpression vector (Fig. 1 B, compare empty vector to $CTS1^{O/E}$, *CTS1* ON, and +Auxin). Notably, this enhanced lethality was only seen in combination with failed septation: WT cells or *inn1-AID* cells in the absence of auxin were not appreciably sensitive to *CTS1* overexpression. In contrast, we found that deleting *CTS1* partially rescued the poor growth of *inn1-AID* strains on auxin-containing media (Fig. 1 C).

Cts1 secretion is blocked in cells with cytokinetic defects

Given that overexpression or absence of Cts1 alters the phenotypic effect of early cytokinesis defects, we sought to determine if the action of this key enzyme in mother–daughter separation is blocked when septation is defective. The RAM network "hippo" signaling system activates transcription of the *CTS1* gene at the M/G1 transition and relieves translational repression of the *CTS1* mRNA (Dohrmann et al., 1992; Jansen et al., 2009). Additionally, Cts1 is a secreted protein that transits the endomembrane system before secretion to the extracellular space (Correa et al., 1982; Elango et al., 1982). Thus, we considered multiple levels at which the function of Cts1 could be regulated in response to septation failure, including *CTS1* gene transcription, mRNA translation, and the Cts1 trafficking before secretion. The *CTS1* mRNA 3′ and 5′ UTRs carry important though incompletely defined regulatory elements (Jansen et al., 2009; Aulds et al., 2012; Wanless et al., 2014). Since N- or C-terminal tagging could disrupt this regulation, we generated a strain expressing Cts1 with an HA-tag internal to the protein. Since *CTS1* expression peaks only briefly following mitotic exit (Mazanka et al., 2008; Brace et al., 2011), we examined *CTS1* mRNA, protein expression, and secretion in a synchronized population of cells undergoing a single cytokinetic event.

We synchronized cells in metaphase, treated them with auxin or vehicle, and then released them from the arrest in the presence

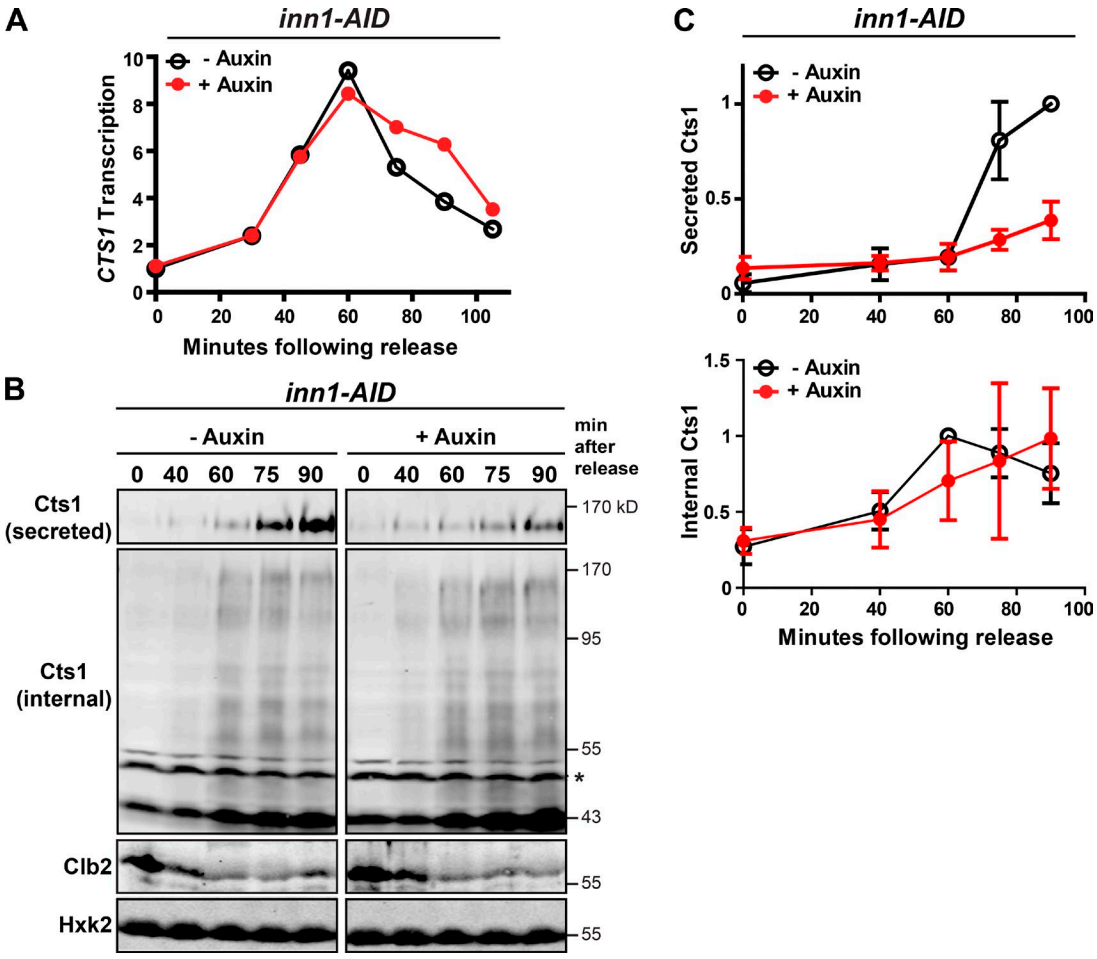

Figure 2. **Septation failure is associated with a block in secretion of the septum degrading enzyme Cts1. (A)** Cts1 transcript induction is not altered upon failed septation. *CTS1* mRNA from cells in B were measured by qPCR at the time indicated after release. The fold change in *CTS1* mRNA (normalized to *ACT1*) relative to −Auxin at time 0 is shown. A representative time course from two independent experiments is shown. **(B)** Cts1 secretion is blocked when septation fails. *inn1-AID* cells expressing HA-tagged Cts1 were synchronized in mitosis and treated with DMSO (−Auxin) or 0.5 mM auxin (+Auxin). Protein was collected at the indicated times following mitotic release at 25°C. A Western blot of secreted Cts1 (top panel) and internal pool of Cts1 (middle panel) is shown. The asterisk indicates a nonspecific band (see Fig. S1 C). Hxk2 and the cyclin Clb2 are shown as a loading and cell cycle release control, respectively (lower panels). A representative blot is shown (see also Fig. S1). **(C)** Western blot quantification. Fold change in the signal of secreted Cts1 (upper panel) and internal Cts1 (lower panel) relative to the maximum signal in the −Auxin control is shown. Error bars represent the SD from three independent time courses.

or absence of auxin. We collected cell samples through a single round of cell division and processed them for RNA, protein, and budding index analysis. We saw no difference in budding index, *CTS1* transcription, translation, or secretion in the presence or absence of auxin in control experiments with WT cells (Fig. S1, C–E). Next, we examined potential regulation of Cts1 during a single cell division event in which cytokinesis was disrupted. Use of the *inn1-AID* genotype allowed us to directly compare the same population of cells with normal (without auxin) or failed septation (with auxin). We observed identical induction of *CTS1* transcription following mitotic exit in cells treated with or without auxin, 0–60 min following release (Fig. 2 A), demonstrating that regulation occurs normally downstream of the transcription factor Ace2.

We then examined Cts1 translation and secretion to the media. Cts1 transits the endomembrane system, where it is heavily O-mannosylated (Kuranda and Robbins, 1991; Gentzsch and Tanner, 1997). Cell lysate (internal fraction) includes nonsecreted Cts1 found in the ER, Golgi, and secretory vesicles and runs as a smear of different glycosylation forms. Cts1 isolated from the media (secreted fraction) runs as the most heavily glycosylated, mature form (Fig. 2 B). We collected cells following metaphase arrest and release and analyzed internal and secreted fractions of Cts1 qualitatively (Fig. 2 B) and quantitatively (Fig. 2 C). During a normal cell division (without auxin), Cts1 (internal) accumulated 40 min following release, peaking at 60 min. After peak internal protein production, secreted Cts1 accumulated in the media (75 min; Fig. 2, B and C, −Auxin).

Under conditions of failed septation (with auxin), the level of internal Cts1 mirrored that of cells undergoing normal cytokinesis (Fig. 2, B and C). Additionally, we saw no obvious change in the glycosylation pattern of internal Cts1 (Fig. 2 B). These data suggest Cts1 cotranslational insertion into the ER and glycosylation are not grossly affected upon failed septation. More strikingly, however, we saw a significant reduction in the amount of Cts1 secreted to the media in cells lacking Inn1. When cytokinesis

proceeded normally, we detected robust Cts1 secretion into the media at 75 min, while finding very little secreted Cts1 at the same time in cells undergoing defective septation (Fig. 2, B and C). Even at a later time point, very little Cts1 was secreted. To confirm this secretion block was due to depleted Inn1 and not auxin treatment we examined Cts1 secretion in auxin-treated *inn1-AID* cells lacking the E3 ligase Tir1 (required for AID-tagged protein degradation) and saw the Cts1 secretion pattern was similar to WT cells and minus auxin samples (Fig. S1 F).

To corroborate these results, we ran a similar experiment in cells expressing an untagged version of Cts1. Using an antibody against the endogenous protein, we found that Cts1 secreted to the media was reduced in cells depleted of Inn1 (Fig. S1 G). This antibody was unfortunately unable to detect the internal fraction of Cts1 (data not shown). Additionally, we measured enzymatic activity of chitinase secreted to the media and found that cells lacking Inn1 exhibited reduced chitinase activity in the cell associated/media fraction compared with control cells (Fig. S1 H). In sum, our findings indicate that transcription, translation, and glycosylation of Cts1 are not grossly affected upon failed septation, but that a significant block in Cts1 secretion occurs.

Identification of a regulatory component monitoring cytokinesis

Our results suggest that cells detect septation defects and block the subsequent step, secretion of chitinase, to ensure the proper order of cell division events. Identification of factors that guarantee the dependency of the system would provide additional evidence of a regulatory system. Cells can rely on an inherent dependency: physically, septum synthesis and degradation cannot occur at the same time, or it could rely on enforcement of a regulatory block to prevent separation until septation is complete. Chitinase overexpression killed cells with disrupted septation, suggesting these processes can occur at the same time. Consequently, we propose the mechanism involves enforcement of a regulatory block and expected elimination of this regulation might cause premature septum degradation and lethality. Thus, we examined high-throughput synthetic genetic array data (Costanzo et al., 2010) to identify gene products demonstrating a negative genetic interaction with known cytokinetic factors. One such gene, *FIR1*, has no known role in cytokinesis yet exhibits negative genetic interactions with several cytokinetic factors, including *GPS1*, *DBF2*, *CYK3*, *FKS1*, and *RGL1*.

Fir1 is a protein with no predicted sizable homology domains and is likely largely an intrinsically disordered protein (IDP). Interestingly, however, Fir1 is highly enriched in short linear motifs (SLiMs), many of which are predicted to mediate protein–protein interactions, protein stability or post-translational modification including sites of Cdk phosphorylation (Holt et al., 2009), and Cdc14-dependent dephosphorylation sites (Kuilman et al., 2015; Fig. S2 A ii). This, together with evidence that *FIR1* transcripts are cell cycle–regulated peaking in G2/M (Spellman et al., 1998) and genome-wide studies demonstrating that Fir1 localizes to the site of septation (Huh et al., 2003), provoked us to further investigate Fir1's role in monitoring the cell division process.

First we determined that elimination of *FIR1* exacerbates the deleterious effect of septation failure. We found that cells carrying *FIR1* deletion divide normally, exhibit WT morphology, and are viable, indicating that the protein is not essential for growth under normal conditions as expected for a canonical checkpoint regulatory protein (Weinert and Hartwell, 1988; Li and Murray, 1991; Fig. 3 A). However, *FIR1* became essential upon failed septation: the *inn1-AID fir1*Δ genotype was lethal with auxin treatment (Fig. 3 A), and loss of *FIR1* was synthetically lethal with other factors that are implicated in cytokinesis and septation, including *CYK3*, *FKS1*, and *RGL1* (Fig. S2 B).

Since cells that fail to complete septation do not secrete Cts1 and are sensitive to inappropriate expression of *CTS1*, we predicted elimination of a regulatory protein might cause premature septum degradation leading to death. Therefore, if the lethal interaction of *FIR1* and *inn1-AID* is due to premature cell separation, it should be suppressed by *CTS1* deletion. We found that *CTS1* deletion restored viability to *inn1-AID fir1*Δ cells treated with auxin (Fig. 3 B). These data support a role for *FIR1* as a regulatory component of a system to monitor septum completion, and that suggests its absence leads to bypass of this system.

Fir1 prevents Cts1 secretion in septation mutants to ensure cell integrity

A block in Cts1 secretion following failure to complete septation (Fig. 2) and genetic evidence demonstrating the lethality of *inn1-AID fir1*Δ cells is reversed by elimination of *CTS1* (Fig. 3 B) suggest that Fir1 functions to block inappropriate Cts1 secretion. To test this directly, we examined Cts1's secretion in *inn1-AID fir1*Δ cells. Concurrently with experiments with *inn1-AID* (Fig. 2), we analyzed and quantified CTS1 transcription (Fig. 3 C), and the production and secretion of Cts1 protein in *inn1-AID fir1*Δ cells (Fig. 3, D and E). We released cells from mitotic arrest in the presence or absence of auxin, and collected samples for RNA and protein analysis. We found *FIR1* deletion did not alter levels of *CTS1* transcription (compare Fig. 2 A and Fig. 3 C), and the onset of transcription (0–60 min) was similar in cells completing cytokinesis normally (–Auxin) and cells failing to complete septation (+Auxin; Fig. 3 C).

Similar to *inn1-AID* cells, *CTS1* translation and glycosylation (internal) were not appreciably altered in the absence of *FIR1* (Fig. 3, D and E). We saw internal production of Cts1 began around 40 min in both auxin-treated and untreated cells and increased over the time course of the experiment. We also did not observe any evidence in overall glycosylation pattern, with a similar smearing and banding pattern in the presence or absence of *FIR1* (compare Fig. 2 B and Fig. 3 D).

However, we saw a marked difference in Cts1 secretion in cells lacking *FIR1*. Unlike *inn1-AID* cells (Fig. 2, B and C), which exhibit reduced Cts1 secretion, auxin-treated *inn1-AID fir1*Δ cells secreted Cts1 to the media at levels comparable to mock-treated cells (Fig. 3, D and E). Interestingly, in the absence of auxin, secreted Cts1 levels began to increase at 60 min (compared with 75 min) in cells lacking *FIR1* compared with WT cells (compare Fig. 2 C and Fig. 3 E, secreted Cts1), suggesting *FIR1* may also play a slight role in preventing premature Cts1 secretion under normal conditions.

To determine if Fir1 monitors the process of septation as opposed to the specific status of Inn1, we generated a GFP- and

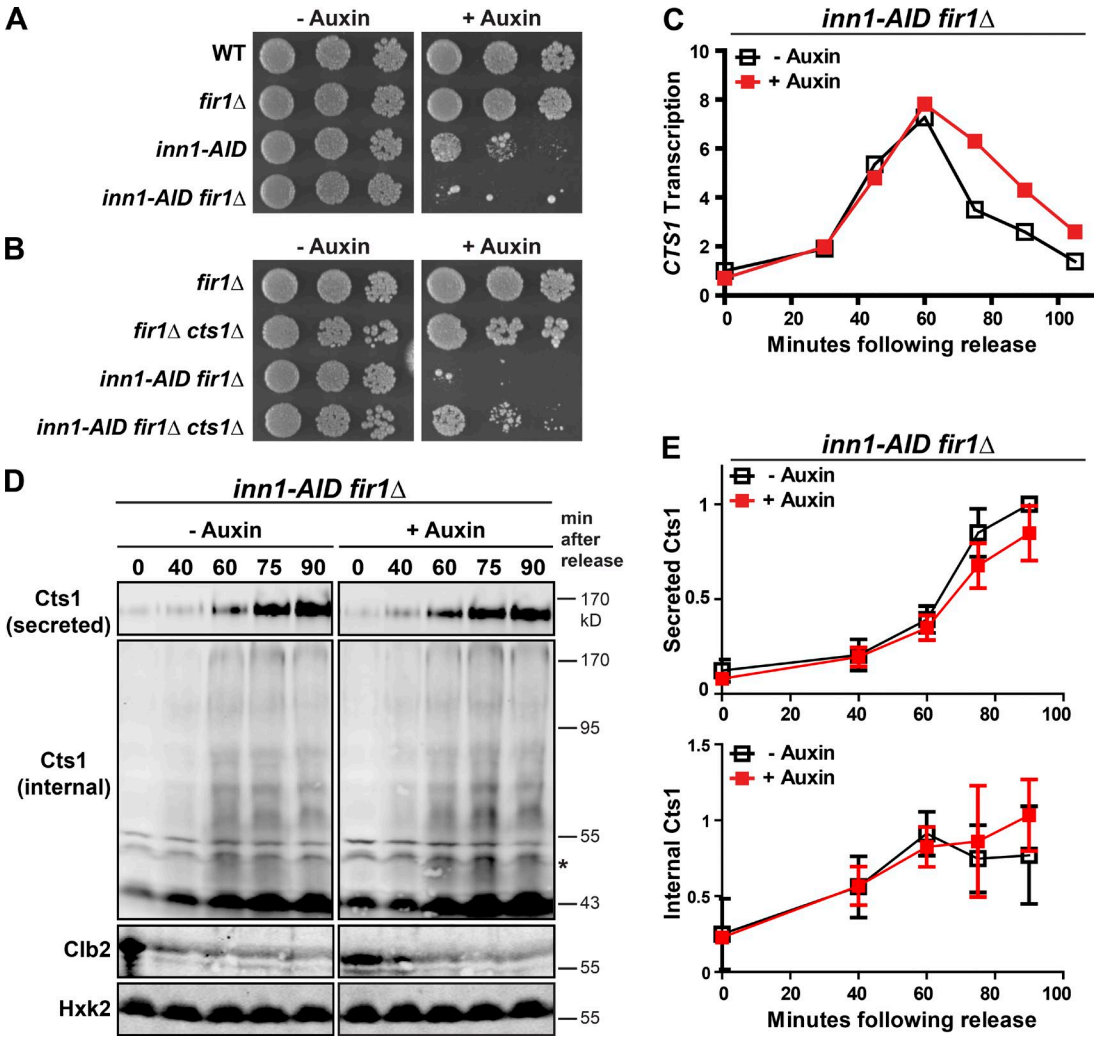

Figure 3. **Septation mutant viability requires Fir1 to prevent inappropriate Cts1 secretion. (A)** Loss of *FIR1* is detrimental to cells with septation defects. Fivefold serial dilutions of the indicated strains were spotted to YPD media as in Fig. 1 C (see also Fig. S2 B). **(B)** *CTS1* deletion rescues the lethality of *inn1-AID fir1Δ*. Fivefold serial dilutions of the indicated strains were spotted to YPD as in Fig. 1 C. **(C)** *CTS1* transcript induction is not altered by lack of *FIR1*. *CTS1* mRNA from cells in D were measured by qPCR as in Fig. 2 A. A representative time course from two independent experiments is shown. **(D)** Fir1 blocks Cts1 secretion when septation fails. *inn1-AID fir1Δ* cells expressing HA-tagged Cts1 were synchronized in mitosis and treated with DMSO (–Auxin) or 0.5 mM auxin (+Auxin). Cells were collected and processed as in Fig. 2 B. **(E)** Western blot quantification (as in Fig. 2 C; Fig. 3, C–E, was done in parallel with Fig. 2, A–C).

degron-tagged allele of Chs2, the enzyme responsible for formation of the primary septum. Cells lacking Chs2 fail to form a primary septum and complete cytokinesis through remedial septum formation (Shaw et al., 1991). As above, we synchronized cells in mitosis, released in the presence or absence of auxin, and monitored Cts1 secretion. Chs2-GFP did not appear at the bud neck in the presence of auxin consistent with its degradation (Fig. 4 A). Cells depleted of Chs2 exhibited markedly reduced secretion of Cts1 without altered levels of internal Cts1 (Fig. 4, B [left] and C). As with loss of Inn1, elimination of *FIR1* in this background restored Cts1 secretion (Fig. 4, B [right] and C). Moreover, we found that *chs2-AID fir1Δ* cells exhibited decreased viability in the presence of auxin compared with *chs2*-AID (Fig. 4 D). Taken together with similar experiments in cells lacking Inn1, these data indicate that Fir1 prevents Cts1 secretion upon failed septation.

Cells that inappropriately secrete Cts1 should lack chitin in the septum and might fail to complete abscission (Cabib and Schmidt, 2003). We treated synchronized WT, *fir1Δ*, *inn1-AID*, and *inn1-AID fir1Δ* cells with auxin or DMSO and pooled time points to enrich for cells that had just failed or completed cytokinesis, respectively. Fixed cells stained with the chitin-binding fluorescent dye calcofluor-white demonstrate the extent of chitin in the bud neck (Pringle, 1991). When septation and cell separation occurred normally (in the absence of auxin or in the presence of auxin where Inn1 is functional), chitin staining was similar in all the genotypes (Fig. 5 A, –Auxin). However, upon auxin addition, *inn1-AID* cells remained attached at the bud neck with strong chitin staining (Fig. 5 A, +Auxin, white triangle). This is consistent with evidence that cells forming a remedial septum contain chitin in the septal region generated by the chitin synthase, Chs3 (Shaw et al., 1991; Cabib and Schmidt, 2003). In contrast, *inn1-AID fir1Δ* cells exhibited extensive regions of chitin-free staining between mother and daughter cells (Fig. 5 A, +Auxin, white arrows). We also noticed several cells forming a

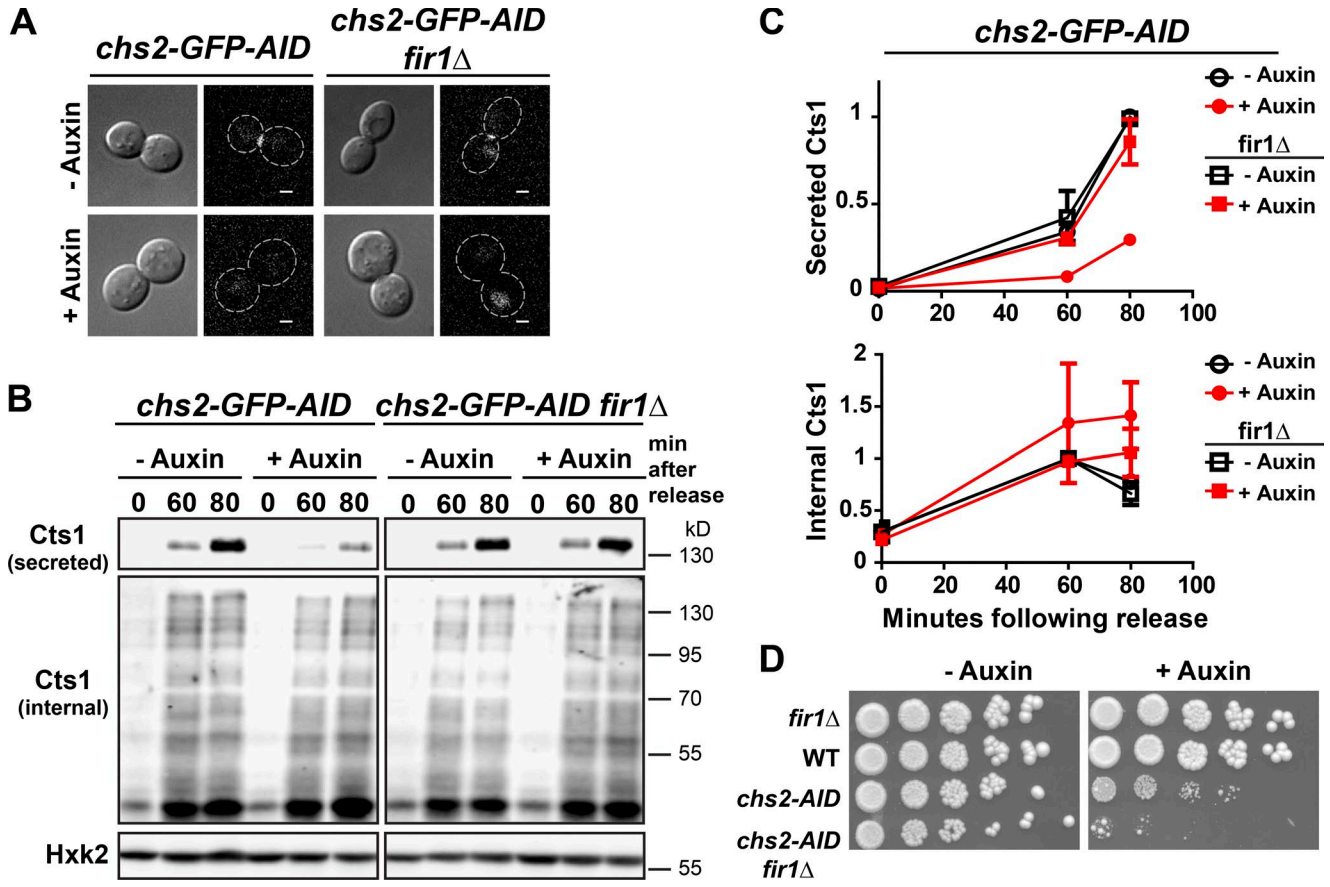

Figure 4. **Fir1 prevents Cts1 secretion upon septation failure.** Inhibition of Cts1 secretion upon septation failure requires Fir1. **(A)** Localization of Chs2-GFP-AID in the presence or absence of auxin. At 30 min after mitotic release, Chs2-GFP-AID localized to the bud neck (−Auxin) while in the presence of auxin (+Auxin) GFP signal at the bud neck could not be detected. A representative cell is shown. Bar, 2 µm. **(B)** *chs2-AID* and *chs2-AID fir1Δ* cells expressing HA-tagged Cts1 were synchronized in mitosis and treated with DMSO (−Auxin) or 0.5 mM auxin (+Auxin). Cells were grown at 27°C, collected, and processed as in Fig. 2 B. **(C)** Western blot quantification (as in Fig. 2 C). **(D)** *FIR1* deletion enhances the lethality of *chs2-AID*. Fivefold serial dilutions of *GalL CDC20 HA-Cts1* strains plus the indicated genotype were spotted to YP galactose plates plus or minus auxin and grown at 27°C.

new bud through the chitin-free region between cells (asterisk) to form a "zygote-like" morphology. To quantify this morphology, we released *inn1-AID* and *inn1-AID fir1Δ* cells from arrest in the presence or absence of auxin and allowed bud formation. Morphology fell into either a chained or zygote-like morphology, and we found a significant increase in the number of zygote-like cells in the *inn1-AID fir1Δ* strain compared with the *inn1-AID* strain (Fig. 5 B). We never saw this phenotype in cells not treated with auxin. Consistent with the hypothesis that cells lacking *FIR1* prematurely degrade the septum as it forms, this zygote-like morphology was observed in cells that lack bud neck chitin through genetic or chemical means of inhibiting chitin synthases (Shaw et al., 1991; Cabib and Schmidt, 2003). We also used expression of a pleckstrin homology (PH) domain fused to GFP, which marks the plasma membrane, to assess cytokinetic plasma membrane closure. This analysis showed that *inn1-AID fir1Δ* cells with wide necks failed to complete closure of the plasma membrane and retained a marked cytoplasmic bridge between mother and daughter cells (Fig. 5 C).

We used electron microscopy to examine septum organization in greater detail. We treated mitotically synchronized *inn1-AID* and *inn1-AID fir1Δ* with DMSO or auxin, released from arrest under corresponding auxin treatment conditions, and collected samples (see Materials and methods). As previously demonstrated (Nishihama et al., 2009), cells lacking *INN1* construct a disorganized, thick remedial septum (Fig. 5 D, +Auxin, top). In the additional absence of *FIR1*, we saw dramatically thinned remedial septa and many cells that failed to complete abscission entirely upon auxin treatment (Fig. 5 D, +Auxin, bottom). Taken together, these data provide additional evidence that Fir1 functions to prevent premature septum degradation upon septation failure.

Cytokinetic defective cells prevent Fir1 degradation

Fir1 localizes to the bud neck (Huh et al., 2003), but its timing and dynamics during cytokinesis are not known. To examine this, we localized Fir1-GFP relative to the AMR component Myo1-mCherry in asynchronous cells. Myo1 marks the site of septation and contracts and disassembles upon completion of septation (Bi et al., 1998). Fir1 initially colocalized with Myo1 in a ring and then filled in a disc-like structure behind the contracting AMR (Fig. 6 A and Video 1). Interestingly, it remained momentarily at the bud neck before its own disappearance. In a population of synchronized cells, we found a similar result: Fir1 and Myo1

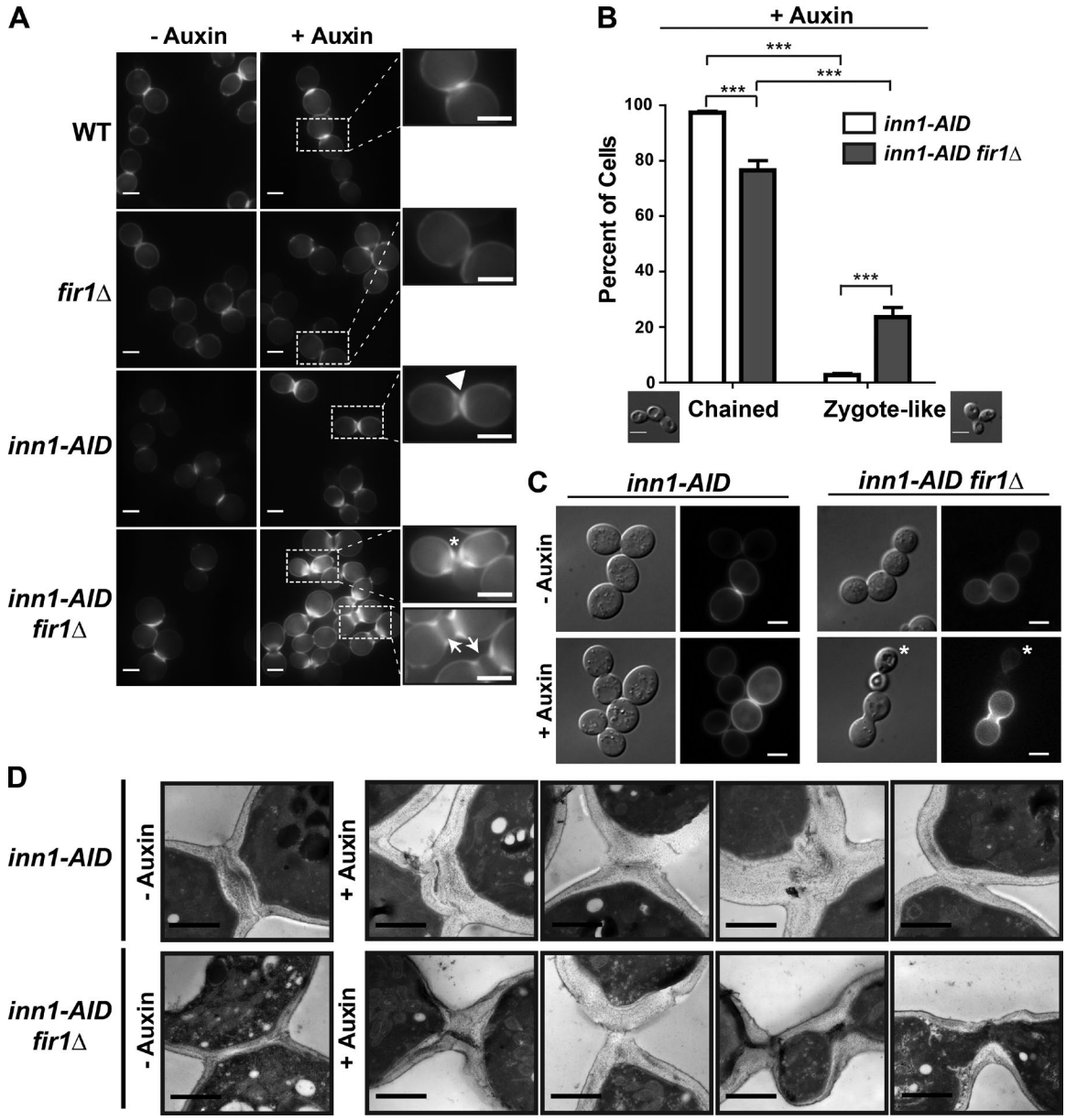

Figure 5. **Inappropriate Cts1 secretion causes premature septum degradation leading to failed abscission and thinned septa. (A)** Inappropriate Cts1 secretion destroys chitin in the aberrant septum. The indicated genotypes, treated with or without auxin, were synchronized and released at 30°C. Cells were collected at times to enrich for cells completing cytokinesis (see Materials and methods). Calcofluor staining of fixed cells demonstrates chitin content. Enlarged region highlights bud neck chitin. Triangle highlights region of increased chitin; arrow, decreased chitin; asterisk, aberrant bud growth. Representative images are shown. Bar, 5 µm. **(B)** Inappropriate secretion of Cts1 leads to failed abscission and budding defects. Synchronized and auxin-treated *inn1-AID* and *inn1-AID fir1Δ* cells were released from arrest at 30°C for 3 h. Budding morphology was binned into chain-like or zygote-like, and the percentage of cells exhibiting the indicated morphology (representative image scale bar, 5 µm) is shown. Error bars represent SD of three independent experiments ($n > 100$ each trial); ***, $P < 0.001$ (two-tailed t test). **(C)** Strains from A were transformed to express the PH-domain of phospholipase C fused to GFP to mark the plasma membrane. Cells were collected as in A, and representative images of the indicated genotype with or without auxin are shown. The asterisk indicates a dead cell. Bar, 5 µm. **(D)** Cells inappropriately secreting Cts1 fail to complete septation or have thinned septal regions. Synchronized *inn1-AID* and *inn1-AID fir1Δ* cells were treated as in A and were processed for electron microscopy. Representative images of each genotype are shown. Bar, 1 µm.

were bud neck–localized in most cells upon early mitotic release (0–20 min), followed by a brief period in which Fir1 was present in more cells than Myo1 (30–45 min), and then neither protein was observed at the bud neck in most cells (45–55 min; Fig. 6 B). When we examined individual cells, Fir1 was present at the bud neck with no detectable Myo1 in 35% ($n = 46$) and 21% ($n = 28$) of cells at 30 min and 40 min, respectively.

Fir1's disappearance from the bud neck could be due to its relocation or degradation. Notably, Fir1, unstable in G1, is a predicted target of the ubiquitin ligases anaphase promoting complex–Cdh1 (Ostapenko et al., 2012) and the Skp1-Cul1-F box–Grr1 (Mark et al., 2014). To determine if Fir1 levels change as cells pass from late mitosis into G1, we synchronized cells by mitotic arrest and release and simultaneously examined Fir1 protein levels, cell separation,

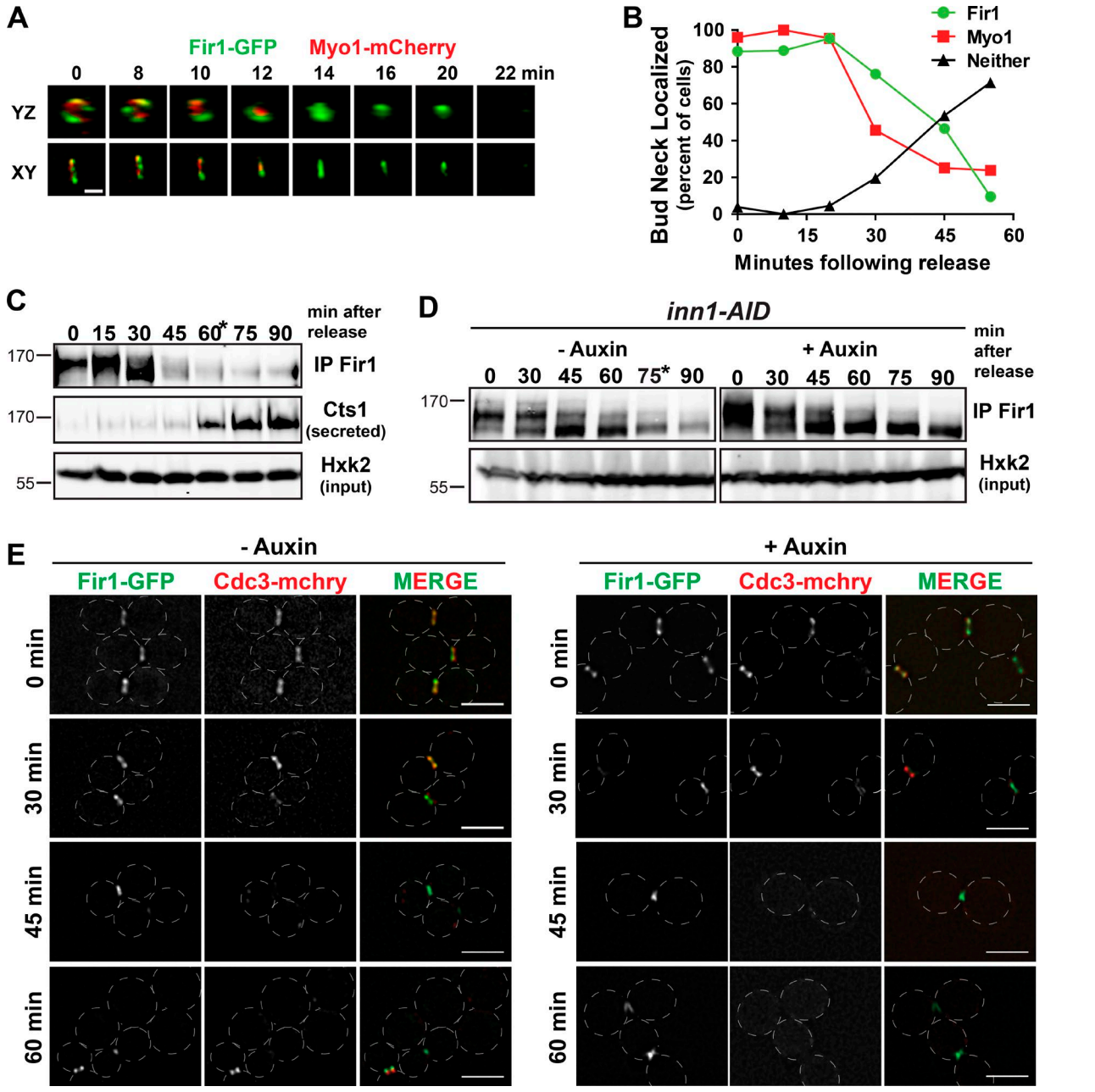

Figure 6. **Fir1 is stabilized at the bud neck when septation is disrupted. (A)** Fir1 localizes to the bud neck in late mitosis. Asynchronous cells expressing Fir1-GFP and Myo1-mCherry were subject to time-lapse microscopy. Maximum projection of serial z-stacks are shown in the xy and yz planes at the times indicated after beginning image acquisition. Bar, 1 µm. A representative cell is shown. See also Video 1. **(B)** Fir1 remains at the site of septation after the completion of cytokinesis. An aliquot of cells from a synchronized population was removed every 10 min after release and was imaged. The percentage of cells with bud neck localization of the indicated protein is shown ($n > 20$ cells per time point). **(C)** Fir1 is degraded before Cts1 secretion. Fir1-myc was immunoprecipitated from normalized lysates (input Hxk2 blot) following release from a synchronized culture at the times indicated at 30°C and subject to immunoblot. From the same culture, secreted Cts1 was collected and subject to immunoblot. A representative blot is shown. The asterisk indicates when peak cell separation was observed (Fig. S3 A). **(D)** Fir1 is not degraded when septation is disrupted. Fir1-myc was immunoprecipitated from normalized lysates (Hxk2 input) in synchronized *inn1-AID* cells treated with or without auxin at 30°C and subject to immunoblot. The asterisk indicates when peak cell separation was observed. Since *inn1-AID* cells treated with auxin do not separate, no asterisk is shown (see Fig. S3B). **(E)** Fir1 remains localized to the bud neck when septation is disrupted. Synchronized *inn1-AID* cells treated with or without auxin were released from arrest, and representative images are shown from the indicated time after release. The septin mCherry-Cdc3 was used to mark the bud neck. Bar, 5 µm (see also Fig. S3, C–E).

and Cts1 secretion. Fir1 exhibited significant electrophoretic shift at mitotic arrest, when CDK activity is high (metaphase/anaphase; T = 0), and lost this shift as cells progressed through mitotic exit (Fig. 6 C). This presumably reflects phosphorylation and dephosphorylation, consistent with evidence that Fir1 is a target of the mitotic CDK (Holt et al., 2009; Kõivomägi et al., 2013) and the phosphatase Cdc14 (Kuilman et al., 2015). At 45 min after release from arrest, the amount of Fir1 present dropped significantly. This loss of Fir1 signal occurred just before peak cell separation (at 60 min, Fig. S3 A) and importantly preceded Cts1 secretion (Fig. 6 C).

To assess the relationship of Fir1's degradation to the start of cell separation (Fig. S3 B), we examined Fir1 levels in *inn1-AID* cells treated with auxin and released from mitotic arrest. Unlike the mock-treated cells, Fir1 levels did not drop appreciably in auxin-treated cells (Fig. 6 D). In contrast, we found that the kinetics of Fir1's loss of electrophoretic mobility shift were unaffected, suggesting efficient dephosphorylation (Fig. 6 D). We saw similar results in cells lacking the cytokinetic factor *CYK3* (Fig. S3 C), indicating that Fir1 stabilization is probably a consequence of cytokinetic failure in cell separation and not specifically due to loss of Inn1.

We next examined Fir1-GFP localization in cells experiencing septation failure. All metaphase-arrested cells had Fir1-GFP at the bud neck. In the absence of auxin, the fraction of large-budded cells with bud neck Fir1-GFP dropped after release from arrest: 53% (n = 80) at 45 min and 31% (n = 91) of large budded cells 60 min after release. In contrast, 75% (n = 96) and 76% (n = 92) of large budded cells treated with auxin at 45 and 60 min retained Fir1 at the bud neck (Fig. 6 E). We also observed Fir1 localizing to the emerging bud in the next cell cycle, a localization pattern that was rarely seen in WT or mock-treated cells (data not shown), consistent with reduced degradation upon failed cytokinesis. We saw a similar result in additional genetic backgrounds that are also defective in cytokinesis (Fig. S3, D and E). Taken together, these data suggest cells with defective septation activate a mechanism to stabilize Fir1 and retain it at the bud neck.

Fir1 may inhibit the cell separation kinase Cbk1

The RAM signaling pathway initiates the cell separation process, and we hypothesized it might be subject to regulation by a septum monitoring system. The downstream-most kinase, Cbk1, acts in a feed-forward loop to promote cell separation by regulating the transcription and translation of cell separation enzymes including *CTS1* (Mazanka et al., 2008; Jansen et al., 2009; Weiss, 2012). To test if elimination of *CBK1* would rescue the *inn1-AID* phenotype, we deleted *CBK1* in the *inn1-AID* strain. As expected, elimination of the kinase that initiates the cell separation process rescued *inn1-AID*'s growth defect (Fig. 7 A). To determine the epistatic relationship between *CBK1* and *FIR1*, we knocked out both genes and found this genotype suppressed the lethality of *inn1-AID* cells, suggesting *CBK1* is epistatic to *FIR1* (Fig. 7 A). These data are likely due to lack of *CTS1* expression in *cbk1*Δ cells; however, we cannot rule out the possibility that *FIR1* may act upstream of *CBK1* to block Cts1 secretion.

Recently, we identified a novel docking motif ([F/Y]XFP) used by Cbk1 to interact with its substrates (Gógl et al., 2015). Fir1 contains two docking motifs matching this consensus, one of which is highly conserved through fungal evolution (Nguyen Ba et al., 2012; Fig. S2 A i). Fir1 robustly coimmunoprecipitated with Cbk1 in vivo (Fig. 7 B; Breitkreutz et al., 2010), and was not pulled down in the absence of *CBK1*. To test if this interaction required intact docking, we mutated the two [F/Y]XFP motifs to AXAP (Fir1 dock*). Fir1 abundance is low in the cell, and we were unable to detect it in cell lysate. Therefore, we verified expression levels upon immunoprecipitation (IP) from normalized lysates (Fig. 7 B). While Fir1 dock* was expressed to a slightly higher level than WT Fir1, elimination of the docking sites strongly reduced its interaction with Cbk1 (Fig. 7 B). Additionally, Fir1 contains several potential Cbk1 consensus phosphorylation sites (Fig. S2, ii) that are also highly conserved through fungal evolution (Mazanka et al., 2008; Nguyen Ba et al., 2012). Fir1 immunoprecipitated from yeast lysate could be phosphorylated by bacterially expressed Cbk1 in vitro, and robust phosphorylation required an intact docking site (Fig. 7 C). Finally, to determine if Fir1's function required its interaction with Cbk1, we examined the growth defect of *inn1-AID* when the endogenous *FIR1* allele was replaced with *fir1 dock**. We found *fir1 dock** did not restore full *FIR1* function to cells failing septation; cells grew more poorly in the presence of auxin exhibiting a phenotype more similar to *inn1-AID fir1*Δ cells (Fig. 7 D). Taken together, these data demonstrate Cbk1 and Fir1 are bona fide interaction partners, and Fir1 function requires binding and/or phosphorylation by Cbk1.

Both Fir1 and Cbk1 localize to the site of septation, and we wondered if altered localization could explain our genetic results. However, Fir1 and Cbk1 localized to the bud neck independently; both proteins were present at the bud neck in the absence of the other (Fig. S4 A). Then, we investigated their dynamics during cytokinesis. We found Fir1 forms a ring at the bud neck before Cbk1's localization to the same ring structure (Fig. 7 E). Then, they fill in a disc-like structure as cells complete cytokinesis (Fig. 7 E and Videos 2 and 3; Mancini Lombardi et al., 2013). To clarify the timing of these proteins during cell separation, we examined localization in a synchronized cell population. At approximately the time of cell separation (50 min), a large proportion of cells (45%, n = 56) exhibited bud neck–localized Cbk1 in the absence of Fir1, suggesting Cbk1 remains at the bud neck after Fir1 degradation (Fig. S4 B).

Cbk1 and the RAM network function to control cell separation. Given Fir1's role in preventing inappropriate separation, we investigated the possibility that Fir1 inhibits Cbk1. Cells lacking functional Cbk1 are unable to degrade the chitin-rich septum (Racki et al., 2000; Bidlingmaier et al., 2001), and cells become "clumpy." Therefore, we hypothesized overexpression of a Cbk1 inhibitor would increase the "clumpiness" or the number of cells connected in a group. WT and *cbk1*Δ cells were transformed with an estradiol-inducible *FIR1* overexpression vector and treated with β-estradiol or vehicle (plus and minus Fir1 overexpression). Upon *FIR1* overexpression (see also Fig. S4 C), cells exhibited a significant increase in the mean number of connected cells per group compared with cells without inducer, similar to cells lacking *CBK1* (Fig. 7 F). Since Cbk1 activates the transcription factor, Ace2, to drive transcription of *CTS1*, we also found *FIR1* overexpression reduced transcript levels of *CTS1* over twofold compared with mock-treated cells (Fig. 7 G). Interestingly, we found *FIR1* overexpression in *cbk1*Δ cells caused a slight but significant increase in the mean number of connected cells per group, suggesting Fir1 may have additional roles in preventing cell separation independent of Cbk1 (Fig. 7 F).

It was recently shown that the protein Lre1 can inhibit Cbk1 in vitro, and may also do so in vivo (Mancini Lombardi et al., 2013). We predicted that eliminating both putative inhibitors (Fir1 and Lre1) would additively increase Cbk1 activity, worsening viability defects of cells with impaired cytokinesis. Thus, we examined growth of *inn1-AID fir1*Δ and *inn1-AID fir1*Δ *lre1*Δ cells in the

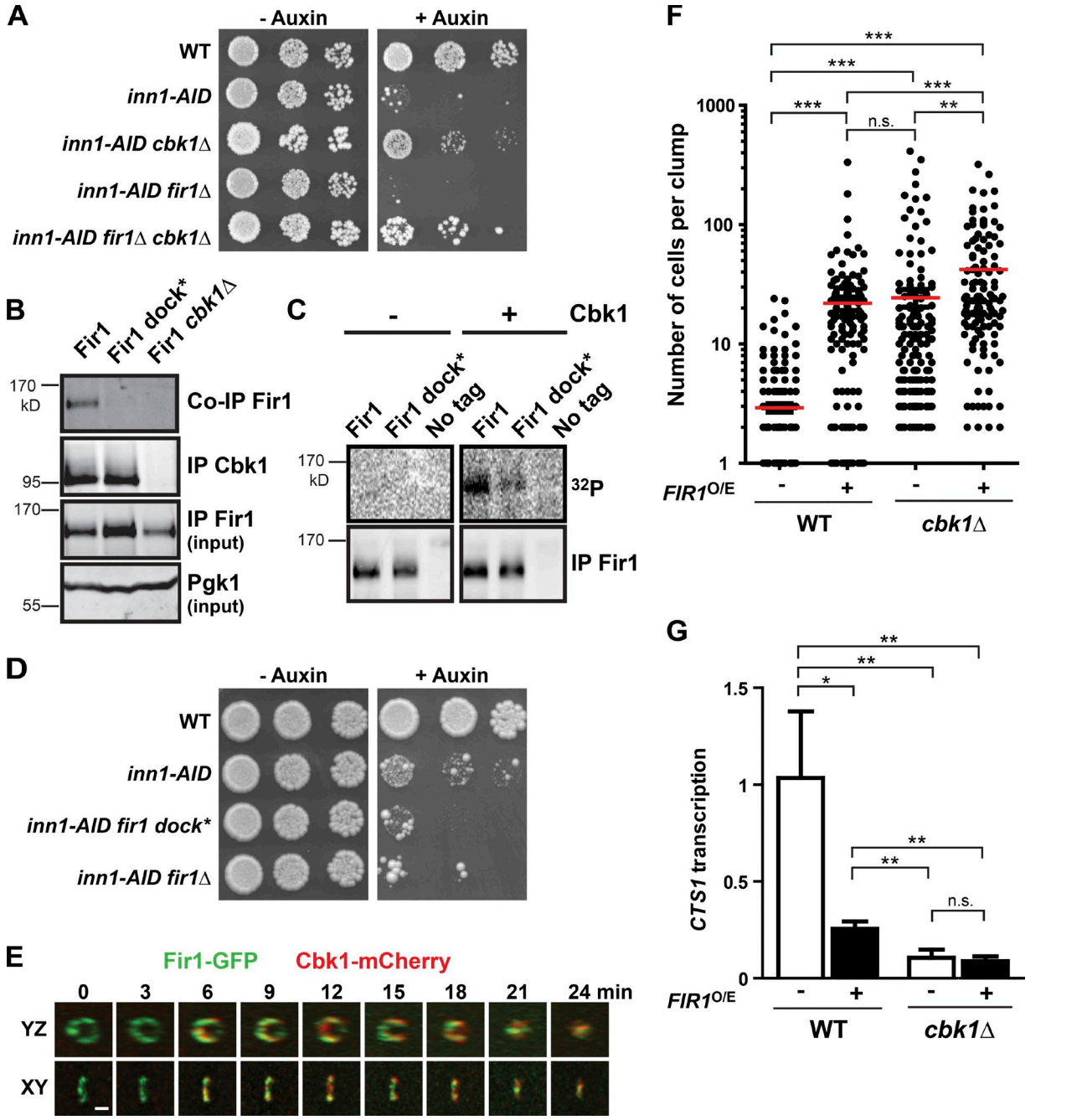

Figure 7. **Fir1 may inhibit separation through inhibition of Cbk1. (A)** *CBK1* deletion rescues the growth defect of cells that fail septation. Fivefold serial dilutions of the indicated strains were spotted to YPD media as in Fig. 1 C. **(B)** Fir1 interaction with Cbk1 in vivo requires Fir1's docking motif. Cbk1 was immunoprecipitated (IP Cbk1) from asynchronous cultures expressing WT Fir1 or the Cbk1 docking motif mutant (Fir1 dock*). Immunoblot of the IP sample demonstrates Fir1 co-IP with Cbk1 (Co-IP Fir1). As a control, cells lacking *CBK1* were subject to the same IP and Western analysis. Total Fir1 (IP Fir1 input) was examined by IP from the same normalized lysate (Pgk1 input). **(C)** Cbk1 phosphorylates Fir1 in vitro. HA-tagged Fir1, Fir1 dock*, or an untagged strain were subject to Fir1 IP from asynchronous culture lysate and treated with or without bacterially purified Cbk1/Mob2 and radiolabeled ^{32}P-ATP. An autoradiograph of Fir1 phosphorylation (upper panel) and an immunoblot showing total Fir1 (lower panel) are shown. **(D)** Fir1 function requires its interaction with Cbk1. Threefold serial dilutions of the indicated strains were spotted to YPD media as in Fig. 1 C (see also Fig. S4 E). **(E)** Cbk1 and Fir1 exhibit unique localization patterns during late mitosis. Synchronized cells expressing Fir1-GFP and Cbk1-3X mCherry were imaged every 3 min. Maximum projection of serial z-stacks is shown in the xy and yz planes at the time indicated after beginning image acquisition. Bar, 1 µm. A representative cell is shown. See also Videos 2 and 3 and Fig. S4, A and B. **(F)** *FIR1* overexpression inhibits cell separation. WT or *cbk1Δ* cells expressing an inducible *FIR1* overexpression vector (see Materials and methods) were grown in the absence or presence of inducer (−/+*FIR1* O/E) at 30°C. The number of connected cells per cell clump (n > 100 clumps) was counted for each sample. The red line indicates the mean clump size for the indicated strain. *, P = 0.01–0.05; **, P = 0.01–0.001; ***, P < 0.001 (one-way ANOVA; see also Fig. S4 C). **(G)** *FIR1* overexpression reduces Ace2 transcriptional output. RNA isolated from the cells in F were subject to qPCR analysis of *CTS1* transcript levels (normalized to *ACT1*). *CTS1* transcript levels are shown relative to *cbk1Δ* cells in the absence of inducer. Mean and SD of three independent experiments are shown. *, P = 0.01–0.05; **, P = 0.01–0.001; n.s. > 0.05 (two-tailed t test).

presence of auxin. We found no genetic interaction between *fir1Δ* and *lre1Δ* in the absence of auxin (no cytokinetic defect; Fig. S4 D). At 30°C, both *inn1-AID fir1Δ* and *inn1-AID fir1Δ lre1Δ* strains grew extremely poorly, preventing meaningful assessment of genetic interaction (Fig. S4 D). However, we found that growth at 37°C partially restored growth defects of *inn1-AID* and *inn1-AID fir1Δ* cells (Fig. S4 D). In contrast, *inn1-AID fir1Δ lre1Δ* cells grew extremely poorly at 37°C, demonstrating a negative genetic interaction between *fir1Δ* and *lre1Δ*. Moreover, combining the *fir1 dock** mutant with *inn1-AID lre1Δ* background demonstrated that the *fir1 dock** allele was unable to restore growth to the *inn1-AID lre1Δ* cells at 37°C (Fig. S4 E), providing additional evidence that a physical association with Cbk1 is required for Fir1 function.

Cbk1 regulates secretion of Cts1

We propose that Fir1 inhibition of Cbk1 helps prevent secretion of Cts1 before completion of septation. However, global inhibition of Cbk1 blocks Ace2-driven gene expression, and we found normal *CTS1* transcription in cells undergoing cytokinetic failure (Fig. 2 C). Thus, Fir1 may act specifically at the bud neck to prevent Cts1 secretion through inhibition of Cbk1, and may not alter Cbk1's ability to activate the transcription factor, Ace2. This model predicts that Cbk1 promotes Cts1 secretion more directly, in addition to its well-established role in activating Ace2 to drive *CTS1* transcription (Racki et al., 2000; Weiss et al., 2002; Mazanka et al., 2008). To test this model, we examined Cts1 secretion in cells lacking *CBK1*. Since *CTS1* is not transcribed in *cbk1Δ* cells (Fig. 7 G; Racki et al., 2000), we replaced the endogenous *ACE2* with a gain-of-function (GOF) *ACE2* allele (*ACE2-GOF*) that mimics Cbk1 phosphorylation by aspartic acid replacement at S122, S137, and S436 (Fig. 8 A; Mazanka et al., 2008). While this strain expresses *CTS1* to a lower level than WT *ACE2*, *CTS1* transcripts are produced with similar timing and levels in both *ACE2-GOF* and *ACE2-GOF cbk1Δ* (Fig. S5 A). We next assessed the production and secretion of Cts1 protein following release from mitosis in the presence and absence of Cbk1. We found that WT and *cbk1Δ* cells carrying the ACE2-GOF allele had no difference in the production of intracellular Cts1 protein (Fig. 8, B and C). However, *cbk1Δ* cells had consistently reduced secretion of Cts1 to the media (Fig. 8, B and C). This result suggests a novel Cbk1 function to promote Cts1 secretion independent of its role in promoting the transcription and translation of *CTS1*.

To validate this function of Cbk1, we also investigated the role of Cbk1 upon cytokinetic failure when *CTS1* is uncoupled from Cbk1 and expressed via the *ACE2-GOF* allele. Arrested *inn1-AID* cells expressing the *ACE2-GOF* allele were treated with or without auxin and released from the arrest, and Cts1 secretion was examined. Cts1 internal production is similar in all strains (Fig. S5 B). As shown previously, cells failing septation do not secrete Cts1 (Fig. 8 D, WT), while cells lacking *FIR1* bypass the block and secrete Cts1 (Fig. 8 D, *fir1Δ*). Importantly, cells lacking *CBK1* secrete very little Cts1 regardless of cytokinesis failure (Fig. 8 D, *cbk1Δ*, +/−Auxin). These data demonstrate functional Cbk1 is required for Cts1 secretion and is consistent with our model that Cbk1 inhibition is important for prevention of Cts1 secretion. Moreover, we find that additionally eliminating *FIR1* only slightly increased the amount of Cts1 secreted to the media (Fig. 8 D, *fir1Δ cbk1Δ*). These data uphold our genetic evidence that *CBK1* is epistatic to *FIR1* and provide additional evidence that Fir1 has only a minor role in preventing Cts1 secretion independent from its inhibition of Cbk1. Consistent with these results, we found *CBK1* deletion rescued the growth defect of *inn1-AID* and *inn1-AID fir1Δ* cells that express *CTS1* independent of *CBK1* (Fig. 8 E). Taken together, these results demonstrate a novel Cbk1 function to promote Cts1 secretion and suggest Fir1 inhibition of Cbk1 could prevent Cts1 secretion when septation is disrupted.

Discussion

Our findings indicate that the final stages of budding yeast cytokinesis are sensitive to the status of the preceding stages of the process. This is manifested by pronounced reduction in secretion of proteins that destroy the septum when septum completion is delayed or disrupted. We propose that a checkpoint-like ECO pathway (Fig. 8 F) maintains the strict temporal sequence of the incompatible stages of cytokinesis: septation and cell separation. Dependency of septum degradation on completion of cytokinesis requires the protein Fir1, which inhibits secretion of the septum degradation enzyme Cts1. Notably, Fir1 is not essential during unperturbed division. Septum completion and abscission appear to trigger destruction of Fir1, relieving the block to septum degradation. Our evidence suggests the ECO pathway blocks premature Cts1 secretion in two distinct ways: by directly inhibiting Cts1 secretion and by inhibiting the protein kinase Cbk1, the Ndr/Lats component of the conserved RAM network "hippo" pathway. We find that Cbk1 is crucial for normal Cts1 secretion septum, a previously unappreciated function that is separate from its well-defined role in activation of *CTS1* transcription. We propose that the ECO pathway functions by stabilizing Fir1 in cells that have not executed septation and abscission, and that completion of these stages of cytokinesis triggers destruction of Fir1 to allow secretion of septum-degrading proteins.

A checkpoint that monitors cytoplasmic separation

Canonically, checkpoints are defined as systems that create and enforce dependency relationships for cell cycle processes in which late events would otherwise occur without regard to completion of earlier ones (Hartwell and Weinert, 1989). The ECO pathway appears to protect budding yeast cytokinesis by ensuring that the onset of cell separation does not occur before septation is complete. In some cases, a checkpoint's action is only strongly evident when the processes it monitors are defective. For example, components of the budding yeast DNA damage and spindle assembly checkpoints are nonessential under ideal growth conditions (Weinert and Hartwell, 1988; Li and Murray, 1991). Cells lacking Fir1 have no pronounced phenotype but are highly sensitive to experimental treatments that disrupt cytokinesis. For example, cells experiencing conditional disruption of septation (*inn1-AID* cells treated with auxin) quickly lose viability in the absence of Fir1, failing to inhibit Cts1 secretion and exhibiting phenotypes consistent with failed cytokinesis and premature septum degradation. How might these experimental conditions reflect challenges to cytokinesis that cells experience under actual growth states? As for genome replication

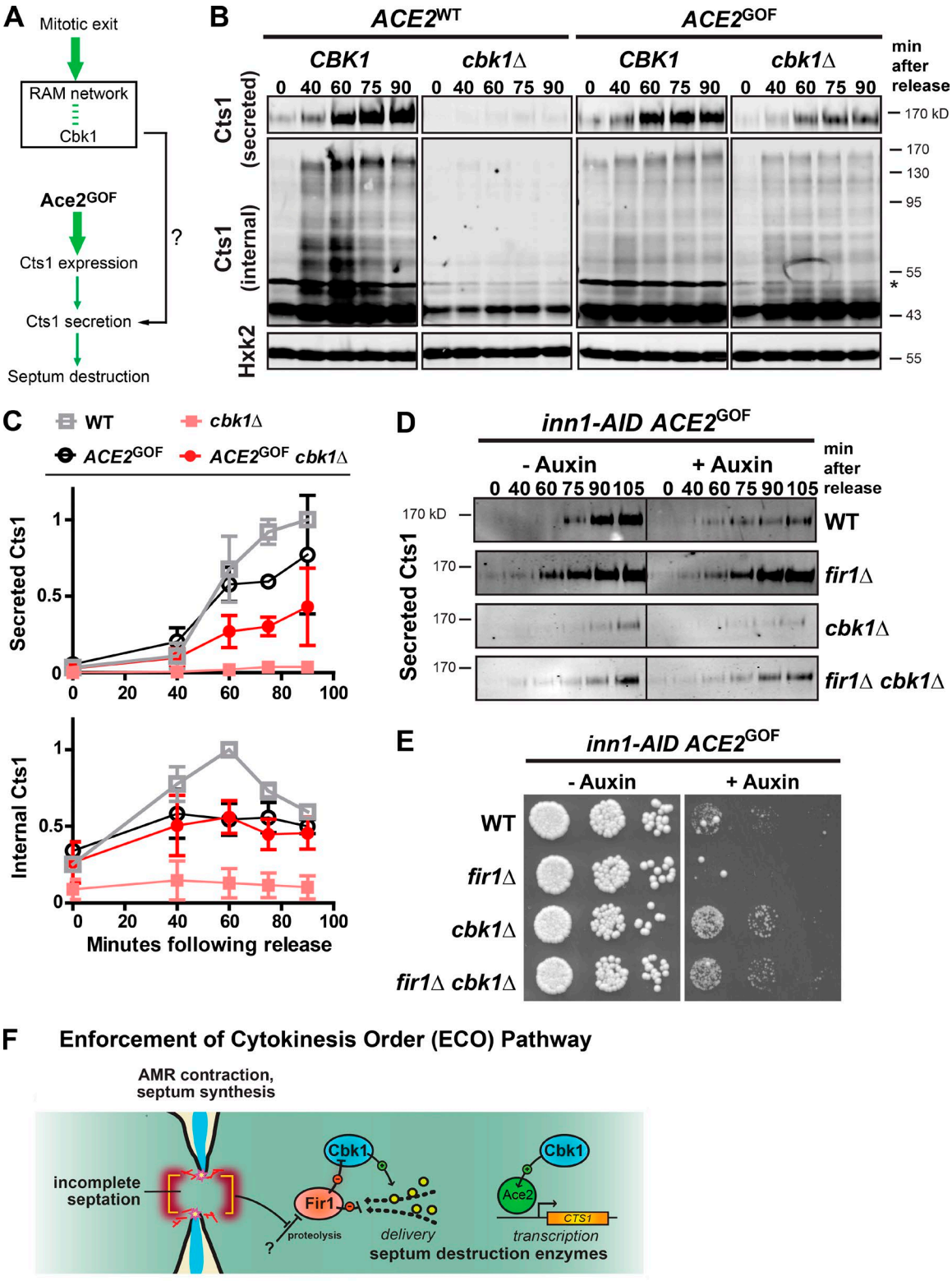

Figure 8. **Cbk1 promotes Cts1 secretion independent of *CTS1* transcription. (A)** Schematic of the *ACE2*-GOF allele bypassing the necessity of Cbk1 to activate *CTS1* transcription. The *ACE2*-GOF allele mimics Cbk1 phosphorylation at S122, S137, and S436 to promote *CTS1* expression in the absence of *CBK1*. **(B)** Cts1 secretion is reduced in the absence of *CBK1* despite normal Cts1 production. WT, *cbk1Δ*, *ACE2*-GOF, *ACE2*-GOF *cbk1Δ* cells expressing HA-tagged Cts1 were synchronized in mitosis. Protein was collected at the indicated times following mitotic release at 30°C and were processed as in Fig. 2 A (see also Fig. S5 A). **(C)** Western blot quantification (as in Fig. 2 B). Fold change relative to the maximum signal of WT cells is shown. **(D)** Fir1 primarily functions to inhibit Cbk1 to prevent Cts1 secretion. *inn1-AID ACE2*-GOF cells with the additional genotype indicated to the right of the panel were treated with DMSO (–Auxin) or 0.5 mM auxin (+Auxin). Secreted protein was collected at the indicated times following mitotic release at 30°C, and a representative Western blot of secreted Cts1 is shown (see also Fig. S5 B). **(E)** Cbk1 deletion restores viability upon septation failure despite Cts1 expression. Fivefold serial dilutions of the strains in

and chromosome segregation, productive division of mother and daughter cells requires temporal orchestration of mechanically disparate processes. In budding yeast, this includes not only localized membrane trafficking and cytoskeleton organization but also coordinated synthesis of extracellular structures from intracellular metabolic precursors that might under some conditions be limited. Systems that ensure cells have time to divide properly when any of the processes involved perform suboptimally could confer significant selective advantage.

Our findings are consistent with prior observations indicating that septum degradation depends on successful execution of cytokinetic abscission and septum completion: specifically, cells that undergo remedial septum formation do not perform mother–daughter separation (Shaw et al., 1991; Bi et al., 1998; Schmidt et al., 2002; Cabib, 2004; Yeong, 2005; Atkins et al., 2013; Onishi et al., 2013). This research broadly hypothesized that the relatively disorganized remedial septum is refractory to separation. However, we find that the remedial septum is destroyed upon ECO bypass. The mechanisms that link ECO to the mechanical progress of cytokinesis are unclear. Intriguingly, cells lacking the AMR component Myo1 exhibit enhanced Cts1 secretion (Ríos Muñoz et al., 2003), and we speculate these cells may fail to activate ECO. Of note, *myo1*Δ cells readily accumulate suppressive aneuploidies (Tolliday et al., 2003; Rancati et al., 2008), consistent with strong selective pressure to combat the detrimental effect of premature septum degradation worsened by loss of mechanisms enforcing the dependency of separation on septation.

Like other checkpoints, the ECO pathway appears to protect cytokinesis by inhibiting a late event (septum degradation) until an earlier one (septation) is completed. Recent work from several laboratories have described elegant mechanisms that also function to ensure order during AMR contraction, septum formation, and bud emergence (Atkins et al., 2013; Meitinger et al., 2013; Onishi et al., 2013; Oh et al., 2017). For example, Cyk3, a protein required for PS formation (early), was demonstrated to inhibit the Rho1 GTPase required for SS formation (late; Onishi et al., 2013). However, we propose here a different mechanism to ensure order. Unlike these other factors, Fir1 does not appear to be required for any step of septation or cell separation. Cells lacking *FIR1* have no obvious phenotype. Instead, Fir1, like other checkpoint proteins, functions to relay information about the status of an early event to a late event. Upon septation failure, Fir1 is stabilized and transmits this information to the RAM network, preventing later processes.

Checkpoints function by monitoring a process and sending a negative signal to block subsequent processes until a particular condition is satisfied. What is the signal that communicates the status of cytokinesis to Fir1? In ECO, we do not yet understand which aspect of septation is being monitored. Cells may monitor defects as cell wall stress via activation of the cell wall integrity pathway (Philip and Levin, 2001), or they may monitor disruptions to the plasma membrane (Kono et al., 2012), or they may monitor a yet unidentified morphological change. Interestingly, decreasing lipid flippase function at the plasma membrane during cytokinesis was shown to suppress the poor growth of septation mutants (Roelants et al., 2015), suggesting that plasma membrane composition changes during cytokinesis could be involved.

The crucial ECO pathway component Fir1 is an IDP with no predicted folded domains but numerous conserved peptide motifs that are known or likely binding partners of folded protein domains (SLiMs; Nguyen Ba et al., 2012). It is becoming clear that IDPs perform diverse important roles, in some cases by generating distinct "phase separated" regions (Wright and Dyson, 2015; Woodruff et al., 2017). Fir1 has an unusually large number of SLiMs (Nguyen Ba et al., 2012), suggesting that it may function as a signaling hub by concentrating multiple interaction sites (Dunker et al., 2005). Intriguingly, rapidly evolving IDPs containing conserved SLiMs and small folded motifs are important in other conserved checkpoints and signaling systems. For example, the Rad9 protein—among the first identified components of the DNA damage checkpoint—is nearly entirely IDP, with a concentration of short BRCT (BRCA1 C terminus) motifs and SLiMs (Weinert and Hartwell, 1988).

How does the ECO pathway protect cytokinesis?

Septation and cell separation in yeast are controlled by two deeply conserved "hippo" pathway signaling systems: the MEN and the RAM networks (Bardin and Amon, 2001; McCollum and Gould, 2001; Weiss, 2012). Response to cytokinesis disruption probably does not involve the MEN, which acts before AMR contraction and septum initiation. We saw no delay of cytokinesis initiation in synchrony experiments, which is inconsistent with MEN inhibition. The RAM network's best-known function in cell separation is activation of Ace2-driven transcription of cell separation genes. Delay of separation could therefore occur by suppression of Ace2 function through RAM network inhibition, as well as through block of cell separation gene translation or delivery of these enzymes to the nascent, unfinished septum. We find that both transcription and translation of the Ace2-driven gene *CTS1* are not affected when cytokinesis is impaired. Rather, cells prevent premature secretion of this enzyme, indicating that the membrane trafficking system is responsive to the status of cytokinesis.

Our findings indicate that the ECO pathway works in part by inhibiting RAM network functions that are independent of Ace2 activation. By unlinking Ace2 function from the RAM network, we were able to determine that secretion of Cts1 is slowed when the RAM network is inhibited, suggesting that RAM plays a role in control of secretion during late cytokinesis. While this could reflect a total block of secretion during cytokinesis, we think this is unlikely. For one, remedial septum synthesis occurring at this time depends on secretion of Chs3 (Cabib and Schmidt, 2003), and we have also found the exocyst component Sec4 relocalized

D (all strains express PrGal-*CDC20 inn1-AID ACE2-GOF TIR1*) were spotted to YP galactose plates with and without the addition of 0.5 mM auxin. Plates were incubated for 2 d at 30°C. **(F)** ECO pathway. Upon incomplete septation, stabilized Fir1 at the bud neck inhibits Cbk1, blocking secretion of septum destroying enzymes. Activation of ECO protects cytokinesis by ensuring the strict temporal sequence of opposing processes: septation and cell separation.

to the bud neck at this time (data not shown). Furthermore, while the RAM network functions in cell growth and morphogenesis in other times during the cell cycle, it is unlikely that the system plays a major role in secretion. The RAM network releases translation repression of proteins that are required for wall expansion during bud growth (Jansen et al., 2009; Wanless et al., 2014). In cells lacking this translation control system, disruption of RAM network function affects maintenance of polarized growth but has no pronounced effect on proliferation or bud growth (Bidlingmaier et al., 2001; Weiss et al., 2002). We therefore propose that the RAM network either promotes default secretion only during septation and cell separation, or specifically activates the trafficking/secretion of specific cargo proteins involved in cell separation. While Cbk1 may regulate glycosylation (Kurischko et al., 2008) we did not find obvious changes in Cts1 glycosylation in cells lacking *CBK1* (Fig. 8 B). Interestingly, the predicted Cbk1 target Boi1 (Gógl et al., 2015) has recently been shown to promote activation of the exocyst (Kustermann et al., 2017; Masgrau et al., 2017). While any requirement for the exocyst in promoting Cts1 secretion is unknown, secretion of septum-destroying enzymes in fission yeast requires functional exocyst (Martín-Cuadrado et al., 2005). Overall, the broader significance of our findings is that trafficking of cytokinetic proteins is precisely timed according to their order of function.

Fir1 is clearly a target of Cbk1 that interacts with the kinase through a conserved docking motif, but the mechanism of inhibition by Fir1 remains unclear. Fir1 lacking functional docking sites did not restore viability to cells failing septation (*inn1-AID* treated with auxin), suggesting inhibition requires this interaction. One possibility is that Fir1 may physically block Cbk1's interaction with other docking motif–containing targets until Fir1 degradation. We have computationally identified potential Cbk1 targets with strong conservation of docking and/or phosphorylation sites (Gógl et al., 2015). Interestingly, while most exhibit conservation of both docking and phosphorylation sites, several lack a conserved docking site. An intriguing possibility is that Fir1 can order Cbk1 substrates by permitting access to some substrates and not others during late stages of cytokinesis. However, we cannot rule out the equally likely, and not mutually exclusive, possibility that Cbk1 phosphorylation of Fir1 plays a more important role in its function. Perhaps phosphorylation of these sites enhances or decreases Fir1's ability to inhibit Cbk1, and this is a key area of further investigation.

How broadly conserved is the ECO pathway?

We suggest that checkpoint-mediated enforcement of dependency in cytokinesis similar to the ECO pathway in overall structure, if not in specific components, is broadly distributed in eukaryotes. Our results are notably consistent with experiments performed in fission yeast: uncoupling the RAM-related pathway, morphogenesis Orb6 network, from upstream controls caused cell lysis. The authors demonstrated that cells failing to inactivate the morphogenesis Orb6 network early during septation prematurely degraded the septum, leading to lethality. Similar to our results here, this phenotype was reversed by deletion of wall-degrading enzymes (Gupta et al., 2014). While fission yeast lacks a sequence homologue of Fir1, a functional orthologue may exist.

Fundamental aspects of cytokinesis are conserved between yeast and animal cells (Balasubramanian et al., 2004; Bhavsar-Jog and Bi, 2017; Glotzer, 2017). Both yeast and metazoan cells undergo cytokinesis through a sequence of coordinated steps that include AMR contraction, membrane ingression, localized secretion, ECM remodeling, and abscission. Mechanisms to ensure coordinated execution of these steps are beginning to be understood (Neto and Gould, 2011; Glotzer, 2017). For example, kinases play a fundamental role in ensuring abscission order (D'Avino and Capalbo, 2016). The polo-like kinase Plk1, activate in late mitosis, prevents the Cep55 protein from prematurely localizing to the midbody. Upon mitotic exit, Plk1 activity drops, and recruitment of Cep55 ensures timely assembly of the machinery required for abscission (Bastos and Barr, 2010). Then Cep55 recruits exocyst components to promote secretion required for abscission (Gromley et al., 2005; Zhao et al., 2006). Remodeling of the extracellular matrix is also important for proper cytokinesis (Hwang et al., 2003; Olson et al., 2006; Xu and Vogel, 2011). However, the dependency relationships between these processes—abscission, localized secretion, and ECM remodeling—are not known. Given the highly conserved nature of many other aspects of cytokinesis, it is interesting to speculate that, like the budding yeast ECO pathway, metazoan cells use similar checkpoint mechanisms to ensure order of these diverse processes.

Materials and methods

Strains, plasmids, and growth conditions

All strains are derived from the W303 genetic background (*leu2-3,112 trp1-1 can1-100 ura3-1 ade2-1 his3-11,15*) and are listed in Table S1. We generated deletion and C-terminal HA, c-Myc (Myc), GFP, and RFP (mCherry)-tagged strains by standard integration methods (Longtine et al., 1998; Sheff and Thorn, 2004). Integration of a 3X-HA internal tag into the Cts1 coding sequence was performed with a pop-in/pop-out method (Schneider et al., 1995) just after the catalytic domain of Cts1 between amino acids A315 and T316. We sequenced the endogenous locus to confirm proper integration. The dual (N- and C-terminally) tagged Fir1 and Fir1 dock* strains were generated by a two-fragment PCR method to replace the *fir1*Δ::KanMX with a PCR amplification of GFP or HA-Fir1 from a plasmid and Fir1-myc::TRP1 from genomic DNA. Untagged *fir1 dock** was integrated at the endogenous locus, replacing a CORE (COunterselectable marker and REporter gene) cassette using the delitto perfetto method (Storici and Resnick, 2006). We sequenced the locus to ensure proper integration. The *ACE2*-GOF (S122D, S137D, and T436D) allele was integrated using a two-fragment PCR method to replace *ace2*Δ::*HIS3* with the GOF allele, a GFP tag and the KanMX marker. The endogenous locus was sequenced to confirm proper integration. The septin Cdc3 was N-terminally tagged upon BglII digest of YIp128-*CDC3*-mCherry (*LEU2*, a gift from E. Bi, University of Pennsylvania, Philadelphia, PA; Gao et al., 2007) and transformation. The plasma membrane marker PH-GFP (LEU2, a gift from Y. Barral, ETH Zurich, Zurich, Switzerland; Mendoza et al., 2009) was transformed into the indicated strains. Derivatives of the *inn1-AID* Pr*ADH1-O.s.TIR1-9MYC* strains were generated by backcrossing to strain YAD236 (a gift from K. Labib, University

of Dundee, Dundee, Scotland; Devrekanli et al., 2012). Genotypes were determined by marker segregation or via PCR confirmation of unmarked alleles (Cts1 internal HA screened with primers: 5′-ATTTGCTAACAAGTGCTAGCCAGAC-3′ and 5′-GATGAAGTT GAGGCTGCTGAGG-3′). Chs2 was C-terminally tagged with GFP and an auxin-inducible degron (Morawska and Ulrich, 2013) and crossed to generate the indicated genotypes. Chs2 degradation was monitored by microscopy.

We generated *CTS1* and *FIR1* overexpression constructs using the drag and drop method (Jansen et al., 2005). Briefly, the coding sequence of *CTS1* or *FIR1* was PCR-amplified with Rec1 and Rec2 overhangs and cotransformed with SalI digested pGREG505::*LEU2* or pGREG575::*LEU2* vectors, respectively. Inserts were integrated into the vector by homologous recombination gap repair. The resulting plasmids were recovered and sequence-confirmed (pELW 2038 and pELW 2039, respectively). The uncut vector served as an empty vector control.

We cultured cells in YP medium (1% yeast extract, 2% peptone; BD Biosciences) containing additional adenine (Ameresco) and 2% glucose (YPD; Millipore) or 2% galactose (YP Gal; MP Biomedical). For microscopy, we used synthetic minimal selection medium (0.67% yeast nitrogen base without amino acids, 0.2% amino acid drop-in; US Biological; and 2% glucose or 2% galactose). Plated media was as above with 2% agar (US Biological). DMSO (0.1% final; Sigma-Aldrich) and auxin (α-naphthalene acetic acid, prepared as a 0.5-M stock in DMSO; HiMedia Laboratories) were added to plates or media at 0.5 mM auxin (0.1% DMSO) final concentration where necessary.

Cell synchrony

For mitotic arrest and release, we grew cells expressing a galactose-inducible GalL-*CDC20* gene to log phase in YP Gal media, washed once with YP media, resuspended in fresh YPD to turn off expression of Cdc20, and arrested in metaphase. We incubated cultures at 30°C until >95% of the cells were large-budded (2.5–3 h). For experiments with *chs2-GFP-AID*, cells were grown at 27°C (we found the phenotype of *chs2-GFP-AID fir1Δ* was enhanced at lower temperatures). For auxin depletion experiments, cultures were split equally and auxin (or DMSO) was added to 0.5 mM final concentration for the last 30–45 min of the arrest. We washed cells twice in YP media (containing auxin or DMSO where necessary) and released them in YP Gal media (containing auxin or DMSO where necessary) at the temperature indicated in the legends of Figs. 2, 3, 4, 6, 8, S1, and S5. At each time point, a sample was removed and the budding index of 100 cells was counted to confirm arrest and release.

Enrichment of cells completing cytokinesis

For Fig. 5 (A, C, and D), we engineered strains to drive induction of GalL-*CDC20* with the addition of deoxycorticosterone (DOC; through DOC-driven activation of Gal4; Picard, 2000). We found this method to improve the timing and synchrony of mitotic release, and the addition of hormone to induce release was advantageous when comparing many strains at once as cells did not require washing before release. We grew cells to log phase in the presence of 50 nM DOC (dissolved in ethanol) and washed three times to remove hormone; in the absence of hormone, *CDC20* is not expressed and cells arrest in metaphase. We incubated cultures at 30°C until >95% of the cells were large-budded (2.5–3 h). Cultures were then split equally, and auxin (or DMSO) was added to a 0.5-mM final concentration for the last 30 min of the arrest. We find most cells that fail septation begin to reinitiate budding at ∼80 min after release and therefore have likely just completed cytokinesis. Therefore, to enrich for cells around this time point, we released cells for 60, 70, and 80 min and mixed them in equal proportions. The mixed population was fixed and processed for chitin staining with calcofluor-white or processed for transmission electron microscopy (TEM) together. Since minus auxin cells complete cytokinesis more rapidly, we combined cells that had been released for 40, 50, and 60 min.

Preparation of secreted and internal Cts1 protein

To examine Cts1 protein production, we synchronized cells as indicated above. At the time points indicated in Figs. 2, 3, 4, 8, S1, and S5, we removed an equivalent number of cells from each culture (typically 2 OD cell equivalents), added sodium azide (to 20-mM final concentration; Sigma-Aldrich), and placed on ice to prevent further protein production or secretion. At the end of the time course, cells were spun down at 20,800 *g* for 1 min, and 90% of the cleared media was added to ice-cold TCA (10% final concentration; Sigma-Aldrich), and we precipitated secreted protein overnight at 4°C. Precipitated protein was pelleted at 20,800 *g* for 15 min at 4°C and washed once in ice-cold acetone (Sigma-Aldrich), and pellets were dried at room temperature. Samples were resuspended in 2× buffered protein loading buffer (125 mM Tris, pH 9.4, 20% glycerol, 4% SDS, 10% 2-mercaptoethanol, and 0.004% bromophenol blue) and boiled at 99°C for 5 min. We ran half of the sample on a 10% SDS-PAGE gel and immunoblotted the gels as indicated below.

We washed the remaining cells in 1.2 M sorbitol and 10 mM Tris, pH 7.6, buffer, and then incubated with 0.5 mg/ml Zymolyase 20T (ICN) in 1.2 M sorbitol, 10 mM Tris, pH 7.6, and 50 mM 2-mercaptoethanol for 30–40 min at 37°C to remove the cell wall. Spheroplasts were gently centrifuged at 830 *g* for 1 min. Cells were lysed on ice by resuspension and brief vortex in 50 mM Tris, pH 7.5, 0.5 mM EDTA, 0.5% Triton X-100, and 1 mM PMSF. We removed cell debris upon centrifugation at 20,800 *g* for 15 min at 4°C. The cleared lysate was added to 2× protein loading buffer (125 mM Tris, pH 6.8, 20% glycerol, 4% SDS, 10% 2-mercaptoethanol, and 0.004% bromophenol blue) and boiled at 99°C for 5 min. Equal volumes (10–20% of the total lysate) were loaded on a 10% SDS-PAGE gel and subjected to immunoblotting as indicated below.

IP

We prepared cell lysate by bead-beating in ice-cold lysis buffer (50 mM Tris-HCl, pH 7.4, 150 mM NaCl, 1% Triton X-100, 10% glycerol, 1 mM dithiothreitol, 120 mM β-glycerolphosphate, 2 mM sodium orthovanadate, 20 mM sodium molybdate, 3 mM benzamidine, 1 mM phenylmehtylsulfonyl fluoride, 1 µg/ml pepstatin, 0.5 mM leupeptin, and 2 µg/ml chymostatin). Anti-HA antibody (12CA5, a gift from R. Lamb) at a 1:50 dilution along with 50 µl of a 1:1 recombinant protein G-Sepharose (Invitrogen) slurry was added to normalized protein, as determined by

Bradford assay (Bio-Rad). We rotated IPs at 4°C for 2 h followed by two washes in ice-cold yeast lysis buffer. We then resuspended the beads in 2× SDS-PAGE sample buffer (125 mM Tris, pH 6.8, 20% glycerol, 4% SDS, 10% 2-mercaptoethanol, and 0.004% bromophenol blue) and resolved the samples on 8% SDS-PAGE gels. Gels were immunblotted as indicated below.

Co-IP

We prepared cell lysates of asynchronous cells by bead-beating in ice-cold lysis buffer (50 mM Tris-HCl, pH 7.4, 150 mM NaCl, 1% Triton X-100, 10% glycerol, 1 mM dithiothreitol, 120 mM β-glycerolphosphate, 2 mM sodium orthovanadate, 20 mM sodium molybdate, 3 mM benzamidine, 1 mM phenylmehtylsulfonyl fluoride, 1 µg/ml pepstatin, 0.5 mM leupeptin, and 2 µg/ml chymostatin). We normalized total protein as determined by Bradford assay (Bio-Rad) and split the lysate equally into two. A sample was removed and added to sample buffer for the input loading control. One aliquot was incubated with anti-HA antibody (12CA5, a gift from R. Lamb) and recombinant protein G-Sepharose (Invitrogen) slurry to determine the total Fir1-HA in the lysate. The other aliquot was incubated with anti-Cbk1 NT5 antibody (Jansen et al., 2006) and recombinant protein G-Sepharose (Invitrogen) slurry for the co-IP. We rotated the beads at 4°C for 2 h followed by three washes in ice-cold yeast lysis buffer. We then resuspended the beads in 2× SDS-PAGE sample buffer (125 mM Tris, pH 6.8, 20% glycerol, 4% SDS, 10% 2-mercaptoethanol, and 0.004% bromophenol blue) and resolved the samples on 8% SDS-PAGE gels. Gels were immunoblotted as described below.

Immunoblotting

For all Western blot assays, we transferred proteins to Immobilon FL polyvinylidene difluoride (Millipore) membrane. Membranes were blocked for 30 min in Odyssey blocking buffer PBS (Licor), then incubated with primary antibody in Tris-buffered saline (50 mM Tris, pH 7.6, and 150 mM NaCl) plus 0.1% Tween (TBST) for 1 h at room temperature or overnight at 4°C. We then incubated blots with secondary antibody in TBST plus 0.1% SDS for 30 min. Membranes were washed three times for 3 min with TBST between antibody additions and before imaging. We used primary antibodies as follows: mouse monoclonal HA antibody (12CA5, a gift from R. Lamb, Northwestern University, Evanston, IL) at 1:1,000, rabbit polyclonal hexokinase (Hxk2; 100-4159; Rockland Immunochemicals) at 1:3,000, rabbit polyclonal Clb2 antibody (y-180; Santa Cruz Biotechnology) at 1:1,000, and rabbit polyclonal chitinase (a gift from S. Strahl, University of Heidelberg, Heidelberg, Germany) at 1:500. We used secondary antibodies as follows: IRDye 680 LT goat anti–mouse (Licor) at 1:20,000 or IRDye 800 CW goat anti–rabbit (Licor) at 1:15,000. We imaged and quantified blots with the Image Studio Lite Odyssey software (v4.0; LiCor), and images of blots were processed using Photoshop (Adobe). We calculated the fold change relative to the maximum signal from the minus auxin control sample for each genotype for each independent time course. Internal Cts1 was additionally normalized by generating a normalization factor from the Hxk2 blot (x/max(x)) and dividing the raw Cts1 value. For Fig. 8, the fold change relative to the maximum signal from WT cells was calculated. In all experiments, the SD from three independent time courses is shown.

Kinase assay

We performed kinase assays as previously described (Jansen et al., 2006). Briefly, we immunoprecipitated Fir1-HA from yeast lysate (see above) and washed the beads three times with kinase reaction buffer (20 mM Tris, pH 8.0, 150 mM NaCl, 5 mM $MnCl_2$, and 20 mM DTT). We resuspended the beads in reaction buffer plus 20 µM cold ATP and 0.33 µCi/µl γ-^{32}P-ATP and added 240 nM bacterially purified Cbk1$^{251–756}$-Mob2 (Gógl et al., 2015). Kinase reactions were allowed to proceed at room temperature for 1 h and stopped by addition of 5× SDS-PAGE sample buffer and 20 min incubation at 80°C. Proteins were separated by 8% SDS-PAGE and transferred to Immobilon FL polyvinylidene difluoride (Millipore) membrane. We visualized ^{32}P using a Storm phosphorimager (GE Biosciences), and total Fir1 was imaged by immunoblotting as described below.

RNA preparation and quantitative RT-PCR

We prepared RNA from synchronized cultures at the times indicated in Figs. 2 and 3 or from the indicated genotype (Figs. 7, S1, and S4) by hot acid phenol extraction as previously described (Collart and Oliviero, 1993).We treated 2 µg of RNA with 10 units of RNase-free DNase I (Roche) and converted it to cDNA with Moloney murine leukemia virus reverse transcription (Promega). We performed quantitative RT-PCRs (qPCR) with the iCycler Thermal Cycler with iQ5 Multicolor Real-Time PCR Detection System (Bio-Rad) using primers specific to *CTS1* and *ACT1* (*CTS1* forward: 5′-TGCACCCAGATTGCTGAA-3′; reverse: 5′-AAACCA TCAACGACTGCTGAG-3′ and *ACT1* forward: 5′-GGTTATTGATAA CGGTTCTGGTATG-3′; reverse: 5′-ATGATACCTTGGTGTCTTGGT CTAC-3′). Efficiencies (E) were obtained by plotting the log of the relative template concentration to the cycle threshold (CT) values from serial dilutions of yeast genomic DNA and calculating $10^{-1/(\text{slope}\ -1)}$. Efficiency-corrected gene expression levels were calculated using the ratio of *CTS1* over *ACT1* with the equation $E^{\Delta CT\ \text{target}\ (T = 0 - T = X\ \text{min sample})}/E^{\Delta CT\ ACT1\ (T = 0 - T = X\ \text{min sample})}$. Fold changes are shown relative to the control sample indicated in the legends of Figs. 2, 3, 7, S1, and S4. A Student's unpaired, two-tailed *t* test was performed using GraphPad Prism version 5.03 to determine significance in Fig. 7. For Figs. 2 and 3, RNA was prepared from two independent experiments, and a representative experiment is shown.

Spot assay, cell separation assays, and morphology assays

For spot assays, we grew cells in YPD to mid–log phase, then normalized to an OD 600 of 0.05 in water. Fivefold or threefold (see legends of Figs. 1, 3, 4, 7, 8, S2, and S4) serial dilutions were made, and 3 µl was spotted onto the plates. We incubated plates for 3–5 d at 30°C (unless otherwise indicated). For cell separation assays, WT or *cbk1*Δ cells were transformed to integrate PYL23 (PrADH1 Gal4 ER VP16) at the *URA3* locus upon digestion with Xcm1 (a gift from F. Cross, Rockefeller University, New York, NY). This generates a strain in which the Gal4 transcription factor is activated upon addition of β-estradiol (Picard, 2000). These strains were then transformed to express FIR1 from the Gal1 promoter (pELW 2039; see above). Finally, the resulting strains were grown in selection media to mid–log phase and diluted again to allow growth to log phase overnight (16 h) in the absence or presence

125 nM β-estradiol (−/+*FIR1* O/E). Samples were randomized, imaged, and analyzed blind. We imaged more than 100 cell clumps per sample, and the number of cells in each clump was plotted. The mean number of cells per clump is indicated as a red line in the figure. One-way ANOVA with Tukey's multiple comparison test was performed using GraphPad Prism version 5.03. Data distribution was assumed to be normal, but this was not formally tested. For zygote-like morphology analysis, cells were arrested in mitosis and released with the addition of 0.5 mM auxin (in DMSO) or DMSO. Cells were grown for an additional 2.5–3 h to allow bud growth, and morphology was binned as chained or zygote-like. Cells were analyzed from three independent experiments in which $n > 100$ cells were counted for each genotype. Significance was determined with an unpaired, two-tailed *t* test using GraphPad Prism version 5.03.

Chitinase enzymatic assay

We washed metaphase-arrested cells three times in fresh media to eliminate previously secreted Cts1. Cells were released into fresh galactose-containing media and grown at 30°C. At the times indicated in the figure, we treated an aliquot of cells with sodium azide (to 10 mM final concentration) and placed it on ice to prevent further secretion. We mixed 30 µl of cells and media with 20 µl of chitinase substrate (250 µM 4-methylumbelliferyl β-D-N,N′,N″-triacetylchitotrioside (Sigma-Aldrich) in 0.25 M sodium citrate, pH 3.0) and incubated the reaction at 30°C for 0, 30, 60, and 90 min. At these times, the reaction was terminated by addition of 50 µl l 0.5 M glycine-NaOH, pH 10.5. Liberated 4-methylumbelliferone (4-MU) was measured with a Synergy 4 microplate reader (BioTek) at an excitation wavelength of 360 nm and an emission wavelength of 450 nm. We used a standard concentration of 4-MU to calculate the activity of chitinase (pmol 4-MU released l/min/cell OD) at each time point after metaphase release.

Calcofluor stain

We fixed the indicated strain with 3.7% formaldehyde and washed twice in PBS (4 mM KH_2PO_4, 16 mM Na_2HPO_4, and 115 mM NaCl, pH 7.3). We resuspended the pellets in 50 µg/ml calcofluor (Sigma-Aldrich), incubated for 5 min at room temperature, and washed an additional two times in PBS. We imaged cells with an Axiovert 200 M microscope (Carl Zeiss; see below), and 0.2-µm z-stack slices were taken. A representative image of the maximum projection for each genotype is shown.

Microscopy and image preparation

We performed microscopy with an Axiovert 200 M microscope, a DeltaVision Core microscope, or a Spinning Disk Confocal system as indicated below. Images of GFP and/or mCherry fused proteins were acquired at room temperature in synthetic minimal medium. We took images in Fig. 5 (A and C), Fig. S1 (A and B), Fig. S3 (B and C), and Fig. S4 A on an Axiovert 200 M microscope fitted with a 100×/1.45 NA oil immersion objective and Cascade II-512B camera (PhotoMetrics, Inc.). Images were acquired using Openlab software (v5.5.0; Improvision), and FIJI and Photoshop (Adobe) were used to make linear adjustments to brightness and contrast. We used the DeltaVision Core fit with a U PLAN S APO 100×, 1.4 NA objective (Olympus), and a CoolSnapHQ2 Camera (Photometrics) for images in Fig. 6 E. A z-series of 0.2-µm step size was taken at the indicated time after release from mitotic arrest. Images were deconvolved using softWoRx's (Applied Precision Ltd.) iterative, constrained three-dimensional deconvolution method. FIJI was used to make linear adjustments to brightness and contrast. A representative single-slice image is shown at each time. We used the Spinning Disk Confocal system (DMI6000 inverted microscope; Leica) fitted with a CSU-X1 spinning disk head (Yokogawa Electric Corp.), a PLAN APO 100×, 1.44 NA objective (Leica), and an Evolve 512 Delta EMCCD camera (Photometrics) for the images in Fig. 6 A and Fig. 7 E. A step size of 0.2 µm was used, and images were acquired using Metamorph (Molecular Devices) and deconvolved using AutoQuant X3's (Media Cybernetics) iterative, constrained three-dimensional deconvolution method. FIJI was used to make linear adjustments to brightness and contrast. A representative maximum projection image is shown.

For TEM, cells were fixed with 2.5% glutaraldehyde in Pipes buffer (0.2 M Pipes, pH 6.8, 0.2 M sorbitol, 2 mM $MgCl_2$, and 2 mM $CaCl_2$) using a PELCO BioWave Microwave Tissue Processor, followed by fixation in 2% potassium permanganate and treatment with 5% uranyl acetate. Ethanol was used for the dehydration series: 30%, 50%, 70%, 90% and 100% (twice). Samples were then embedded in LR white resin, and 90-nm sections were cut using a diamond knife on an Ultracut S Ultramicrotome. Sections were post-stained with uranyl acetate and lead citrate before imaging in the JEOL 1230 TEM (equipped with a Gatan Orius SC1000 CCD camera) with an 80-kV accelerating voltage. The DeltaVision Core, Spinning Disk Confocal system, and JEOL 1230 TEM microscopes are housed in the Northwestern Biological Imaging Facility supported by the Northwestern University Office for Research.

Online supplemental material

Fig. S1 shows control *inn1-AID* experimentation. Fig. S2 shows a schematic of Fir1 and Fir1 genetic interactions. Fig. S3 shows Fir1 stabilization in additional cytokinetic mutants. Fig. S4 shows data supporting Fir1 inhibition of Cbk1. Fig. S5 shows control experiments with the *ACE2-GOF* allele. Table S1 lists strains used in this study. Video 1 shows live-cell imaging of Fir1 and Myo1. Videos 2 and 3 show live-cell imaging of Fir1 and Cbk1.

Acknowledgments

We thank members of the Weiss and L. Lackner laboratories at Northwestern University for critical review of the manuscript. We thank K. Labib, G. Pereria (German Cancer Research Center, Heidelberg, Germany), F. Cross, E. Bi, R. Lamb, Y. Barral, and S. Strahl for strains, plasmids, and antibodies. We thank C. Wilke (Northwestern University, Biological Imaging Facility) for assistance with electron microscopy and E. Anderson and S. Zdraljevic (Northwestern University) for assistance with R software (statistical analysis and graphing). We also thank staff and instrumentation assistance from Northwestern University's Biological Imaging Facility, which is supported by the Chemistry for Life Processes Institute and the Northwestern Office for Research,

and from the Northwestern University's High Throughput Analysis Laboratory, which is a core facility of the Lurie Cancer Center (grant #P30CA060553) .

Research reported in this publication was supported by the National Institute of General Medical Sciences of the National Institutes of Health under award number R01GM084223 to E.L. Weiss. The content is solely the responsibility of the authors and does not necessarily represent the official views of the National Institutes of Health.

The authors declare no competing financial interests.

Author contributions: conceptualization, J.L. Brace and E.L. Weiss; methodology, J.L. Brace and E.L. Weiss; investigation, J.L. Brace, M.D. Doerfler, and E.L. Weiss; writing, J.L. Brace and E.L. Weiss; visualization, J.L. Brace and E.L. Weiss; and funding acquisition, E.L. Weiss.

Submitted: 17 May 2018
Revised: 28 August 2018
Accepted: 5 October 2018

References

Atkins, B.D., S. Yoshida, K. Saito, C.F. Wu, D.J. Lew, and D. Pellman. 2013. Inhibition of Cdc42 during mitotic exit is required for cytokinesis. *J. Cell Biol.* 202:231–240. https://doi.org/10.1083/jcb.201301090

Aulds, J., S. Wierzbicki, A. McNairn, and M.E. Schmitt. 2012. Global identification of new substrates for the yeast endoribonuclease, RNase mitochondrial RNA processing (MRP). *J. Biol. Chem.* 287:37089–37097. https://doi.org/10.1074/jbc.M112.389023

Balasubramanian, M.K., E. Bi, and M. Glotzer. 2004. Comparative analysis of cytokinesis in budding yeast, fission yeast and animal cells. *Curr. Biol.* 14:R806–R818. https://doi.org/10.1016/j.cub.2004.09.022

Bardin, A.J., and A. Amon. 2001. Men and sin: what's the difference? *Nat. Rev. Mol. Cell Biol.* 2:815–826. https://doi.org/10.1038/35099020

Bastos, R.N., and F.A. Barr. 2010. Plk1 negatively regulates Cep55 recruitment to the midbody to ensure orderly abscission. *J. Cell Biol.* 191:751–760. https://doi.org/10.1083/jcb.201008108

Bhavsar-Jog, Y.P., and E. Bi. 2017. Mechanics and regulation of cytokinesis in budding yeast. *Semin. Cell Dev. Biol.* 66:107–118. https://doi.org/10.1016/j.semcdb.2016.12.010

Bi, E., P. Maddox, D.J. Lew, E.D. Salmon, J.N. McMillan, E. Yeh, and J.R. Pringle. 1998. Involvement of an actomyosin contractile ring in Saccharomyces cerevisiae cytokinesis. *J. Cell Biol.* 142:1301–1312. https://doi.org/10.1083/jcb.142.5.1301

Bidlingmaier, S., E.L. Weiss, C. Seidel, D.G. Drubin, and M. Snyder. 2001. The Cbk1p pathway is important for polarized cell growth and cell separation in Saccharomyces cerevisiae. *Mol. Cell. Biol.* 21:2449–2462. https://doi.org/10.1128/MCB.21.7.2449-2462.2001

Brace, J., J. Hsu, and E.L. Weiss. 2011. Mitotic exit control of the Saccharomyces cerevisiae Ndr/LATS kinase Cbk1 regulates daughter cell separation after cytokinesis. *Mol. Cell. Biol.* 31:721–735. https://doi.org/10.1128/MCB.00403-10

Breitkreutz, A., H. Choi, J.R. Sharom, L. Boucher, V. Neduva, B. Larsen, Z.-Y. Lin, B.-J. Breitkreutz, C. Stark, G. Liu, et al. 2010. A global protein kinase and phosphatase interaction network in yeast. *Science.* 328:1043–1046. https://doi.org/10.1126/science.1176495

Cabib, E. 2004. The septation apparatus, a chitin-requiring machine in budding yeast. *Arch. Biochem. Biophys.* 426:201–207. https://doi.org/10.1016/j.abb.2004.02.030

Cabib, E., and M. Schmidt. 2003. Chitin synthase III activity, but not the chitin ring, is required for remedial septa formation in budding yeast. *FEMS Microbiol. Lett.* 224:299–305. https://doi.org/10.1016/S0378-1097(03)00477-4

Cabib, E., S.J. Silverman, and J.A. Shaw. 1992. Chitinase and chitin synthase 1: counterbalancing activities in cell separation of Saccharomyces cerevisiae. *J. Gen. Microbiol.* 138:97–102. https://doi.org/10.1099/00221287-138-1-97

Chin, C.F., A.M. Bennett, W.K. Ma, M.C. Hall, and F.M. Yeong. 2012. Dependence of Chs2 ER export on dephosphorylation by cytoplasmic Cdc14 ensures that septum formation follows mitosis. *Mol. Biol. Cell.* 23:45–58. https://doi.org/10.1091/mbc.e11-05-0434

Collart, M.A., and S. Oliviero. 1993. Preparation of Yeast RNA. *Curr. Protoc. Mol. Biol.* 13:13.12.

Colman-Lerner, A., T.E. Chin, and R. Brent. 2001. Yeast Cbk1 and Mob2 activate daughter-specific genetic programs to induce asymmetric cell fates. *Cell.* 107:739–750. https://doi.org/10.1016/S0092-8674(01)00596-7

Correa, J.U., N. Elango, I. Polacheck, and E. Cabib. 1982. Endochitinase, a mannan-associated enzyme from Saccharomyces cerevisiae. *J. Biol. Chem.* 257:1392–1397.

Cortés, J.C.G., M. Sato, J. Muñoz, M.B. Moreno, J.A. Clemente-Ramos, M. Ramos, H. Okada, M. Osumi, A. Durán, and J.C. Ribas. 2012. Fission yeast Ags1 confers the essential septum strength needed for safe gradual cell abscission. *J. Cell Biol.* 198:637–656. https://doi.org/10.1083/jcb.201202015

Costanzo, M., A. Baryshnikova, J. Bellay, Y. Kim, E.D. Spear, C.S. Sevier, H. Ding, J.L.Y. Koh, K. Toufighi, S. Mostafavi, et al. 2010. The genetic landscape of a cell. *Science.* 327:425–431. https://doi.org/10.1126/science.1180823

D'Avino, P.P., and L. Capalbo. 2016. Regulation of midbody formation and function by mitotic kinases. *Semin. Cell Dev. Biol.* 53:57–63. https://doi.org/10.1016/j.semcdb.2016.01.018

Devrekanli, A., M. Foltman, C. Roncero, A. Sanchez-Diaz, and K. Labib. 2012. Inn1 and Cyk3 regulate chitin synthase during cytokinesis in budding yeasts. *J. Cell Sci.* 125:5453–5466. https://doi.org/10.1242/jcs.109157

Dohrmann, P.R., G. Butler, K. Tamai, S. Dorland, J.R. Greene, D.J. Thiele, and D.J. Stillman. 1992. Parallel pathways of gene regulation: homologous regulators SWI5 and ACE2 differentially control transcription of HO and chitinase. *Genes Dev.* 6:93–104. https://doi.org/10.1101/gad.6.1.93

Dunker, A.K., M.S. Cortese, P. Romero, L.M. Iakoucheva, and V.N. Uversky. 2005. Flexible nets. The roles of intrinsic disorder in protein interaction networks. *FEBS J.* 272:5129–5148. https://doi.org/10.1111/j.1742-4658.2005.04948.x

Elango, N., J.U. Correa, and E. Cabib. 1982. Secretory character of yeast chitinase. *J. Biol. Chem.* 257:1398–1400.

Gao, X.-D., L.M. Sperber, S.A. Kane, Z. Tong, A.H.Y. Tong, C. Boone, and E. Bi. 2007. Sequential and distinct roles of the cadherin domain-containing protein Axl2p in cell polarization in yeast cell cycle. *Mol. Biol. Cell.* 18:2542–2560. https://doi.org/10.1091/mbc.e06-09-0822

Gentzsch, M., and W. Tanner. 1997. Protein-O-glycosylation in yeast: protein-specific mannosyltransferases. *Glycobiology.* 7:481–486. https://doi.org/10.1093/glycob/7.4.481

Glotzer, M. 2017. Cytokinesis in metazoa and fungi. *Cold Spring Harb. Perspect. Biol.* 9:a022343. https://doi.org/10.1101/cshperspect.a022343

Gógl, G., K.D. Schneider, B.J. Yeh, N. Alam, A.N. Nguyen Ba, A.M. Moses, C. Hetényi, A. Reményi, and E.L. Weiss. 2015. The structure of an NDR/LATS kinase–Mob complex reveals a novel kinase–coactivator system and substrate docking mechanism. *PLoS Biol.* 13:e1002146. https://doi.org/10.1371/journal.pbio.1002146

Gould, G.W. 2016. Animal cell cytokinesis: The role of dynamic changes in the plasma membrane proteome and lipidome. *Semin. Cell Dev. Biol.* 53:64–73. https://doi.org/10.1016/j.semcdb.2015.12.012

Green, R.A., E. Paluch, and K. Oegema. 2012. Cytokinesis in animal cells. *Annu. Rev. Cell Dev. Biol.* 28:29–58. https://doi.org/10.1146/annurev-cellbio-101011-155718

Gromley, A., C. Yeaman, J. Rosa, S. Redick, C.T. Chen, S. Mirabelle, M. Guha, J. Sillibourne, and S.J. Doxsey. 2005. Centriolin anchoring of exocyst and SNARE complexes at the midbody is required for secretory-vesicle-mediated abscission. *Cell.* 123:75–87. https://doi.org/10.1016/j.cell.2005.07.027

Gupta, S., M. Govindaraghavan, and D. Mccollum. 2014. Crosstalk between NDR kinase pathways coordinates cytokinesis with cell separation in Schizosaccharomyces pombe. *Eukaryot. Cell.* 13:1104–1112. https://doi.org/10.1128/EC.00129-14

Hartwell, L.H. 1971. Genetic control of the cell division cycle in yeast. IV. Genes controlling bud emergence and cytokinesis. *Exp. Cell Res.* 69:265–276. https://doi.org/10.1016/0014-4827(71)90223-0

Hartwell, L.H., and T.A. Weinert. 1989. Checkpoints: controls that ensure the order of cell cycle events. *Science.* 246:629–634.

Holt, L.J., B.B. Tuch, J. Villén, A.D. Johnson, S.P. Gygi, and D.O. Morgan. 2009. Global analysis of Cdk1 substrate phosphorylation sites provides in-

sights into evolution. *Science.* 325:1682–1686. https://doi.org/10.1126/science.1172867

Huh, W.-K., J.V. Falvo, L.C. Gerke, A.S. Carroll, R.W. Howson, J.S. Weissman, and E.K. O'Shea. 2003. Global analysis of protein localization in budding yeast. *Nature.* 425:686–691. https://doi.org/10.1038/nature02026

Hwang, H.-Y., S.K. Olson, J.D. Esko, and H.R. Horvitz. 2003. Caenorhabditis elegans early embryogenesis and vulval morphogenesis require chondroitin biosynthesis. *Nature.* 423:439–443. https://doi.org/10.1038/nature01634

Jansen, G., C. Wu, B. Schade, D.Y. Thomas, and M. Whiteway. 2005. Drag&-Drop cloning in yeast. *Gene.* 344:43–51. https://doi.org/10.1016/j.gene.2004.10.016

Jansen, J.M., M.F. Barry, C.K. Yoo, and E.L. Weiss. 2006. Phosphoregulation of Cbk1 is critical for RAM network control of transcription and morphogenesis. *J. Cell Biol.* 175:755–766. https://doi.org/10.1083/jcb.200604107

Jansen, J.M., A.G. Wanless, C.W. Seidel, and E.L. Weiss. 2009. Cbk1 regulation of the RNA-binding protein Ssd1 integrates cell fate with translational control. *Curr. Biol.* 19:2114–2120. https://doi.org/10.1016/j.cub.2009.10.071

Juanes, M.A., and S. Piatti. 2016. The final cut: cell polarity meets cytokinesis at the bud neck in S. cerevisiae. *Cell. Mol. Life Sci.* 73:3115–3136. https://doi.org/10.1007/s00018-016-2220-3

Khodjakov, A., and C.L. Rieder. 2009. The nature of cell-cycle checkpoints: facts and fallacies. *J. Biol.* 8:88. https://doi.org/10.1186/jbiol195

Kõivomägi, M., M. Ord, A. Iofik, E. Valk, R. Venta, I. Faustova, R. Kivi, E.R.M. Balog, S.M. Rubin, and M. Loog. 2013. Multisite phosphorylation networks as signal processors for Cdk1. *Nat. Struct. Mol. Biol.* 20:1415–1424. https://doi.org/10.1038/nsmb.2706

Kono, K., Y. Saeki, S. Yoshida, K. Tanaka, and D. Pellman. 2012. Proteasomal degradation resolves competition between cell polarization and cellular wound healing. *Cell.* 150:151–164. https://doi.org/10.1016/j.cell.2012.05.030

Kuilman, T., A. Maiolica, M. Godfrey, N. Scheidel, R. Aebersold, and F. Uhlmann. 2015. Identification of Cdk targets that control cytokinesis. *EMBO J.* 34:81–96. https://doi.org/10.15252/embj.201488958

Kuranda, M.J., and P.W. Robbins. 1991. Chitinase is required for cell separation during growth of Saccharomyces cerevisiae. *J. Biol. Chem.* 266:19758–19767.

Kurischko, C., G. Weiss, M. Ottey, and F.C. Luca. 2005. A role for the Saccharomyces cerevisiae regulation of Ace2 and polarized morphogenesis signaling network in cell integrity. *Genetics.* 171:443–455. https://doi.org/10.1534/genetics.105.042101

Kurischko, C., V.K. Kuravi, N. Wannissorn, P.A. Nazarov, M. Husain, C. Zhang, K.M. Shokat, J.M. McCaffery, and F.C. Luca. 2008. The yeast LATS/Ndr kinase Cbk1 regulates growth via Golgi-dependent glycosylation and secretion. *Mol. Biol. Cell.* 19:5559–5578. https://doi.org/10.1091/mbc.e08-05-0455

Kustermann, J., Y. Wu, L. Rieger, D. Dedden, T. Phan, P. Walther, A. Dünkler, and N. Johnsson. 2017. The cell polarity proteins Boi1p and Boi2p stimulate vesicle fusion at the plasma membrane of yeast cells. *J. Cell Sci.* 130:2996–3008. https://doi.org/10.1242/jcs.206334

Lesage, G., and H. Bussey. 2006. Cell wall assembly in Saccharomyces cerevisiae. *Microbiol. Mol. Biol. Rev.* 70:317–343. https://doi.org/10.1128/MMBR.00038-05

Levin, D.E. 2005. Cell wall integrity signaling in Saccharomyces cerevisiae. *Microbiol. Mol. Biol. Rev.* 69:262–291. https://doi.org/10.1128/MMBR.69.2.262-291.2005

Li, R., and A.W. Murray. 1991. Feedback control of mitosis in budding yeast. *Cell.* 66:519–531. https://doi.org/10.1016/0092-8674(81)90015-5

Longtine, M.S., A. McKenzie III, D.J. Demarini, N.G. Shah, A. Wach, A. Brachat, P. Philippsen, and J.R. Pringle. 1998. Additional modules for versatile and economical PCR-based gene deletion and modification in Saccharomyces cerevisiae. *Yeast.* 14:953–961. https://doi.org/10.1002/(SICI)1097-0061(199807)14:10%3C953::AID-YEA293%3E3.0.CO;2-U

Mancini Lombardi, I., S. Palani, F. Meitinger, Z. Darieva, A. Hofmann, A.D. Sharrocks, and G. Pereira. 2013. Lre1 directly inhibits the NDR/Lats kinase Cbk1 at the cell division site in a phosphorylation-dependent manner. *Curr. Biol.* 23:1736–1745. https://doi.org/10.1016/j.cub.2013.07.032

Mark, K.G., M. Simonetta, A. Maiolica, C.A. Seller, and D.P. Toczyski. 2014. Ubiquitin ligase trapping identifies an SCF(Saf1) pathway targeting unprocessed vacuolar/lysosomal proteins. *Mol. Cell.* 53:148–161. https://doi.org/10.1016/j.molcel.2013.12.003

Martín-Cuadrado, A.B., J.L. Morrell, M. Konomi, H. An, C. Petit, M. Osumi, M. Balasubramanian, K.L. Gould, F. Del Rey, and C.R. de Aldana. 2005. Role of septins and the exocyst complex in the function of hydrolytic enzymes responsible for fission yeast cell separation. *Mol. Biol. Cell.* 16:4867–4881. https://doi.org/10.1091/mbc.e04-12-1114

Masgrau, A., A. Battola, T. Sanmartin, L.P. Pryszcz, T. Gabaldón, and M. Mendoza. 2017. Distinct roles of the polarity factors Boi1 and Boi2 in the control of exocytosis and abscission in budding yeast. *Mol. Biol. Cell.* 28:3082–3094. https://doi.org/10.1091/mbc.e17-06-0404

Mazanka, E., J. Alexander, B.J. Yeh, P. Charoenpong, D.M. Lowery, M. Yaffe, and E.L. Weiss. 2008. The NDR/LATS family kinase Cbk1 directly controls transcriptional asymmetry. *PLoS Biol.* 6:e203. https://doi.org/10.1371/journal.pbio.0060203

McCollum, D., and K.L. Gould. 2001. Timing is everything: regulation of mitotic exit and cytokinesis by the MEN and SIN. *Trends Cell Biol.* 11:89–95. https://doi.org/10.1016/S0962-8924(00)01901-2

Meitinger, F., B. Petrova, I.M. Lombardi, D.T. Bertazzi, B. Hub, H. Zentgraf, and G. Pereira. 2010. Targeted localization of Inn1, Cyk3 and Chs2 by the mitotic-exit network regulates cytokinesis in budding yeast. *J. Cell Sci.* 123:1851–1861. https://doi.org/10.1242/jcs.063891

Meitinger, F., S. Palani, and G. Pereira. 2012. The power of MEN in cytokinesis. *Cell Cycle.* 11:219–228. https://doi.org/10.4161/cc.11.2.18857

Meitinger, F., H. Richter, S. Heisel, B. Hub, W. Seufert, and G. Pereira. 2013. A safeguard mechanism regulates Rho GTPases to coordinate cytokinesis with the establishment of cell polarity. *PLoS Biol.* 11:e1001495. https://doi.org/10.1371/journal.pbio.1001495

Mendoza, M., C. Norden, K. Durrer, H. Rauter, F. Uhlmann, and Y. Barral. 2009. A mechanism for chromosome segregation sensing by the NoCut checkpoint. *Nat. Cell Biol.* 11:477–483. https://doi.org/10.1038/ncb1855

Mierzwa, B., and D.W. Gerlich. 2014. Cytokinetic abscission: molecular mechanisms and temporal control. *Dev. Cell.* 31:525–538. https://doi.org/10.1016/j.devcel.2014.11.006

Morawska, M., and H.D. Ulrich. 2013. An expanded tool kit for the auxin-inducible degron system in budding yeast. *Yeast.* 30:341–351. https://doi.org/10.1002/yea.2967

Musacchio, A. 2015. The Molecular Biology of Spindle Assembly Checkpoint Signaling Dynamics. *Curr. Biol.* 25:R1002–R1018. https://doi.org/10.1016/j.cub.2015.08.051

Nähse, V., L. Christ, H. Stenmark, and C. Campsteijn. 2017. The Abscission Checkpoint: Making It to the Final Cut. *Trends Cell Biol.* 27:1–11. https://doi.org/10.1016/j.tcb.2016.10.001

Nelson, B., C. Kurischko, J. Horecka, M. Mody, P. Nair, L. Pratt, A. Zougman, L.D.B. McBroom, T.R. Hughes, C. Boone, and F.C. Luca. 2003. RAM: a conserved signaling network that regulates Ace2p transcriptional activity and polarized morphogenesis. *Mol. Biol. Cell.* 14:3782–3803. https://doi.org/10.1091/mbc.e03-01-0018

Neto, H., and G.W. Gould. 2011. The regulation of abscission by multi-protein complexes. *J. Cell Sci.* 124:3199–3207. https://doi.org/10.1242/jcs.083949

Nguyen Ba, A.N., B.J. Yeh, D. van Dyk, A.R. Davidson, B.J. Andrews, E.L. Weiss, and A.M. Moses. 2012. Proteome-wide discovery of evolutionary conserved sequences in disordered regions. *Sci. Signal.* 5:rs1. https://doi.org/10.1126/scisignal.2002515

Nishihama, R., J.H. Schreiter, M. Onishi, E.A. Vallen, J. Hanna, K. Moravcevic, M.F. Lippincott, H. Han, M.A. Lemmon, J.R. Pringle, and E. Bi. 2009. Role of Inn1 and its interactions with Hof1 and Cyk3 in promoting cleavage furrow and septum formation in S. cerevisiae. *J. Cell Biol.* 185:995–1012. https://doi.org/10.1083/jcb.200903125

Nishimura, K., T. Fukagawa, H. Takisawa, T. Kakimoto, and M. Kanemaki. 2009. An auxin-based degron system for the rapid depletion of proteins in nonplant cells. *Nat. Methods.* 6:917–922. https://doi.org/10.1038/nmeth.1401

Norden, C., M. Mendoza, J. Dobbelaere, C.V. Kotwaliwale, S. Biggins, and Y. Barral. 2006. The NoCut pathway links completion of cytokinesis to spindle midzone function to prevent chromosome breakage. *Cell.* 125:85–98. https://doi.org/10.1016/j.cell.2006.01.045

Oh, Y., K.-J. Chang, P. Orlean, C. Wloka, R. Deshaies, and E. Bi. 2012. Mitotic exit kinase Dbf2 directly phosphorylates chitin synthase Chs2 to regulate cytokinesis in budding yeast. *Mol. Biol. Cell.* 23:2445–2456. https://doi.org/10.1091/mbc.e12-01-0033

Oh, Y., J.H. Schreiter, H. Okada, C. Wloka, S. Okada, D. Yan, X. Duan, and E. Bi. 2017. Hof1 and Chs4 Interact via F-BAR Domain and Sel1-like Repeats to Control Extracellular Matrix Deposition during Cytokinesis. *Curr. Biol.* 27:2878–2886.e5. https://doi.org/10.1016/j.cub.2017.08.032

Olson, S.K., J.R. Bishop, J.R. Yates, K. Oegema, and J.D. Esko. 2006. Identification of novel chondroitin proteoglycans in Caenorhabditis elegans: embryonic cell division depends on CPG-1 and CPG-2. *J. Cell Biol.* 173:985–994. https://doi.org/10.1083/jcb.200603003

Onishi, M., N. Ko, R. Nishihama, and J.R. Pringle. 2013. Distinct roles of Rho1, Cdc42, and Cyk3 in septum formation and abscission during yeast cytokinesis. *J. Cell Biol.* 202:311–329. https://doi.org/10.1083/jcb.201302001

Ostapenko, D., J.L. Burton, and M.J. Solomon. 2012. Identification of anaphase promoting complex substrates in S. cerevisiae. *PLoS One.* 7:e45895. https://doi.org/10.1371/journal.pone.0045895

Palani, S., F. Meitinger, M.E. Boehm, W.D. Lehmann, and G. Pereira. 2012. Cdc14-dependent dephosphorylation of Inn1 contributes to Inn1-Cyk3 complex formation. *J. Cell Sci.* 125:3091–3096. https://doi.org/10.1242/jcs.106021

Philip, B., and D.E. Levin. 2001. Wsc1 and Mid2 are cell surface sensors for cell wall integrity signaling that act through Rom2, a guanine nucleotide exchange factor for Rho1. *Mol. Cell. Biol.* 21:271–280. https://doi.org/10.1128/MCB.21.1.271-280.2001

Picard, D. 2000. Posttranslational regulation of proteins by fusions to steroid-binding domains. *Methods Enzymol.* 327:385–401. https://doi.org/10.1016/S0076-6879(00)27291-1

Pringle, J.R. 1991. Staining of bud scars and other cell wall chitin with calcofluor. *Methods Enzymol.* 194:732–735. https://doi.org/10.1016/0076-6879(91)94055-H

Proctor, S.A., N. Minc, A. Boudaoud, and F. Chang. 2012. Contributions of turgor pressure, the contractile ring, and septum assembly to forces in cytokinesis in fission yeast. *Curr. Biol.* 22:1601–1608. https://doi.org/10.1016/j.cub.2012.06.042

Racki, W.J., A.M. Bécam, F. Nasr, and C.J. Herbert. 2000. Cbk1p, a protein similar to the human myotonic dystrophy kinase, is essential for normal morphogenesis in Saccharomyces cerevisiae. *EMBO J.* 19:4524–4532. https://doi.org/10.1093/emboj/19.17.4524

Rancati, G., N. Pavelka, B. Fleharty, A. Noll, R. Trimble, K. Walton, A. Perera, K. Staehling-Hampton, C.W. Seidel, and R. Li. 2008. Aneuploidy underlies rapid adaptive evolution of yeast cells deprived of a conserved cytokinesis motor. *Cell.* 135:879–893. https://doi.org/10.1016/j.cell.2008.09.039

Ríos Muñoz, W., M. Irizarry Ramírez, F. Rivera Molina, S. González Crespo, and J.R. Rodríguez-Medina. 2003. Myosin II is important for maintaining regulated secretion and asymmetric localization of chitinase 1 in the budding yeast Saccharomyces cerevisiae. *Arch. Biochem. Biophys.* 409:411–413. https://doi.org/10.1016/S0003-9861(02)00614-8

Roelants, F.M., B.M. Su, J. von Wulffen, S. Ramachandran, E. Sartorel, A.E. Trott, and J. Thorner. 2015. Protein kinase Gin4 negatively regulates flippase function and controls plasma membrane asymmetry. *J. Cell Biol.* 208:299–311. https://doi.org/10.1083/jcb.201410076

Sanchez-Diaz, A., V. Marchesi, S. Murray, R. Jones, G. Pereira, R. Edmondson, T. Allen, and K. Labib. 2008. Inn1 couples contraction of the actomyosin ring to membrane ingression during cytokinesis in budding yeast. *Nat. Cell Biol.* 10:395–406. https://doi.org/10.1038/ncb1701

Schmidt, M., B. Bowers, A. Varma, D.-H. Roh, and E. Cabib. 2002. In budding yeast, contraction of the actomyosin ring and formation of the primary septum at cytokinesis depend on each other. *J. Cell Sci.* 115:293–302.

Schneider, B.L., W. Seufert, B. Steiner, Q.H. Yang, and A.B. Futcher. 1995. Use of polymerase chain reaction epitope tagging for protein tagging in Saccharomyces cerevisiae. *Yeast.* 11:1265–1274. https://doi.org/10.1002/yea.320111306

Shaw, J.A., P.C. Mol, B. Bowers, S.J. Silverman, M.H. Valdivieso, A. Durán, and E. Cabib. 1991. The function of chitin synthases 2 and 3 in the Saccharomyces cerevisiae cell cycle. *J. Cell Biol.* 114:111–123. https://doi.org/10.1083/jcb.114.1.111

Sheff, M.A., and K.S. Thorn. 2004. Optimized cassettes for fluorescent protein tagging in Saccharomyces cerevisiae. *Yeast.* 21:661–670. https://doi.org/10.1002/yea.1130

Spellman, P.T., G. Sherlock, M.Q. Zhang, V.R. Iyer, K. Anders, M.B. Eisen, P.O. Brown, D. Botstein, and B. Futcher. 1998. Comprehensive identification of cell cycle-regulated genes of the yeast Saccharomyces cerevisiae by microarray hybridization. *Mol. Biol. Cell.* 9:3273–3297. https://doi.org/10.1091/mbc.9.12.3273

Steigemann, P., C. Wurzenberger, M.H. Schmitz, M. Held, J. Guizetti, S. Maar, and D.W. Gerlich. 2009. Aurora B-mediated abscission checkpoint protects against tetraploidization. *Cell.* 136:473–484. https://doi.org/10.1016/j.cell.2008.12.020

Storici, F., and M.A. Resnick. 2006. The delitto perfetto approach to in vivo site-directed mutagenesis and chromosome rearrangements with synthetic oligonucleotides in yeast. *Methods Enzymol.* 409:329–345. https://doi.org/10.1016/S0076-6879(05)09019-1

Tolliday, N., M. Pitcher, and R. Li. 2003. Direct evidence for a critical role of myosin II in budding yeast cytokinesis and the evolvability of new cytokinetic mechanisms in the absence of myosin II. *Mol. Biol. Cell.* 14:798–809. https://doi.org/10.1091/mbc.e02-09-0558

VerPlank, L., and R. Li. 2005. Cell cycle-regulated trafficking of Chs2 controls actomyosin ring stability during cytokinesis. *Mol. Biol. Cell.* 16:2529–2543. https://doi.org/10.1091/mbc.e04-12-1090

Wanless, A.G., Y. Lin, and E.L. Weiss. 2014. Cell morphogenesis proteins are translationally controlled through UTRs by the Ndr/LATS target Ssd1. *PLoS One.* 9:e85212. https://doi.org/10.1371/journal.pone.0085212

Weinert, T.A., and L.H. Hartwell. 1988. The RAD9 gene controls the cell cycle response to DNA damage in Saccharomyces cerevisiae. *Science.* 241:317–322. https://doi.org/10.1126/science.3291120

Weiss, E.L. 2012. Mitotic exit and separation of mother and daughter cells. *Genetics.* 192:1165–1202. https://doi.org/10.1534/genetics.112.145516

Weiss, E.L., C. Kurischko, C. Zhang, K. Shokat, D.G. Drubin, and F.C. Luca. 2002. The Saccharomyces cerevisiae Mob2p-Cbk1p kinase complex promotes polarized growth and acts with the mitotic exit network to facilitate daughter cell-specific localization of Ace2p transcription factor. *J. Cell Biol.* 158:885–900. https://doi.org/10.1083/jcb.200203094

Woodruff, J.B., B. Ferreira Gomes, P.O. Widlund, J. Mahamid, A. Honigmann, and A.A. Hyman. 2017. The Centrosome Is a Selective Condensate that Nucleates Microtubules by Concentrating Tubulin. *Cell.* 169:1066–1077.e10. https://doi.org/10.1016/j.cell.2017.05.028

Wright, P.E., and H.J. Dyson. 2015. Intrinsically disordered proteins in cellular signalling and regulation. *Nat. Rev. Mol. Cell Biol.* 16:18–29. https://doi.org/10.1038/nrm3920

Xu, X., and B.E. Vogel. 2011. A secreted protein promotes cleavage furrow maturation during cytokinesis. *Curr. Biol.* 21:114–119. https://doi.org/10.1016/j.cub.2010.12.006

Yeong, F.M. 2005. Severing all ties between mother and daughter: cell separation in budding yeast. *Mol. Microbiol.* 55:1325–1331. https://doi.org/10.1111/j.1365-2958.2005.04507.x

Zhang, G., R. Kashimshetty, K.E. Ng, H.B. Tan, and F.M. Yeong. 2006. Exit from mitosis triggers Chs2p transport from the endoplasmic reticulum to mother-daughter neck via the secretory pathway in budding yeast. *J. Cell Biol.* 174:207–220. https://doi.org/10.1083/jcb.200604094

Zhao, W.M., A. Seki, and G. Fang. 2006. Cep55, a microtubule-bundling protein, associates with centralspindlin to control the midbody integrity and cell abscission during cytokinesis. *Mol. Biol. Cell.* 17:3881–3896. https://doi.org/10.1091/mbc.e06-01-0015